Intracranial EEG Phantom for Brain Stimulation Studies

Final Report

BME 400

14 December 2025

Clients: Dr. Raheel Ahmed, Dr. Arun Manattu

UW School of Medicine and Public Health

Neurosurgery

Advisor: Dr. Paul Campagnola

University of Wisconsin–Madison

Department Chair of Biomedical Engineering

Section 303

Avery Schuda (Team Leader) - aschuda@wisc.edu

Lilly MacKenzie (Communicator) - lfmackenzie@wisc.edu

Orla Ryan (BWIG)- orryan@wisc.edu

Helene Schroeder (BSAC) - hschroeder4@wisc.edu

Corissa Hutmaker (BPAG) - hutmaker@wisc.edu

Abstract

Epilepsy is a prevalent neurological condition marked by the occurrence of repeated, uncontrollable seizures. This disorder can present in individuals of all ages, but commonly manifests in children. One main treatment method is that of surgical intervention, in which neurosurgeons identify and disconnect cranial regions involved in seizure generation; before operation, brain mapping techniques such as intracranial electroencephalography (iEEG) and transcranial magnetic stimulation (TMS) are utilized to delineate brain connectivity. Investigating the safety of using these methods in tandem is to be completed via the fabrication of a brain phantom model. The prototype decided upon involves a hydrogel brain encased in clear resin that can be stimulated to depict any effects of TMS pulses on iEEG electrodes. After considering various criteria, such as substance reactivity and associated preparation techniques, the FormLabs BioMed Clear resin was selected to comprise the skull, while two hydrogel options are still being considered: an agar-based solution and a gelatin-based solution. Preliminary testing was performed to delineate both hydrogels mechanically and thermally; however, due to several inconsistencies in results and noted potential sources of error, a large focus this upcoming semester will be further characterizing each option, focusing mainly on thermal and electrical conductivity. Obtaining physiological accuracy will, in part, be supplemented using both pediatric magnetic resonance imaging (MRI) and computed tomography (CT) scans. After deciding upon the most appropriate brain tissue representative, a final model will be constructed. Finally, the end goal is to stimulate the completed model, including inserted iEEG electrodes, TMS pulses to observe any indication of electrode displacement, temperature change, or induced currents.

Table of Contents

I. Introduction

Motivation

There are a range of neurological disorders, each capable of causing a profound impact on an individual's life. Epilepsy, as the fourth most common neurological disorder, is characterized by the regular appearance of uncontrollable seizures. These seizures occur as a result of short, excessive electrical discharge in neurons and can either be focal in nature, involving a local neuronal network, or generalized, engaging a larger bilateral network, as displayed in Figure 1. This disorder can be detrimental to one's ability to thrive, and is associated with a higher risk of depression, accidents, and death. People of all ages can be affected by epilepsy, but it often manifests before the age of one year [1]. Despite this broad demographic, there is a significant lack of research and clinical explorations in pediatric patients, possibly due to the complicated ethical challenges surrounding the participation of children in human studies [2].

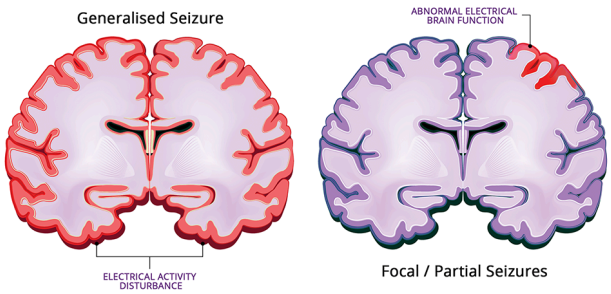

Figure 1: Neuronal recruitment in focal and generalized seizures [3].

The obstacles that impede research studies utilizing pediatric participants may result in a gap of treatment knowledge. As such, constructing study tools that can spur on discoveries targeted towards this younger population is of great importance. An area of exploration tied to epilepsy is that of various treatment methods. Aside from the use of medication, surgical management is an oft-investigated treatment tool in the control of epileptic seizures. Prior to surgical intervention, which may involve procedures such as temporal lobectomies, or removal of certain portions of the brain, a variety of brain mapping techniques such as intracranial electroencephalography (iEEG) and transcranial magnetic stimulation (TMS) are utilized to provide a guide for neurosurgeons. These techniques, involving implanted electrodes and applied magnetic simulation, respectively, have been tested on phantom models before being applied to human subjects to certify their level of risk and effectiveness [4].

Existing Devices

While there exist brain phantoms that have been used for similar research, none meet all of the specifications required by this project, particular in reference to the pediatric-focused research question Dr. Ahmed seeks to address. Researchers at the University of Iowa created a

gel-based brain phantom to prove that TMS and iEEG can be safely used in tandem, specifically in adult patients. The brain of this phantom was made of poly(acrylic acid) (PAA) saline gel, and the skull was made of poly(methyl methacrylate) (PMMA), which is displayed in Figure 2.

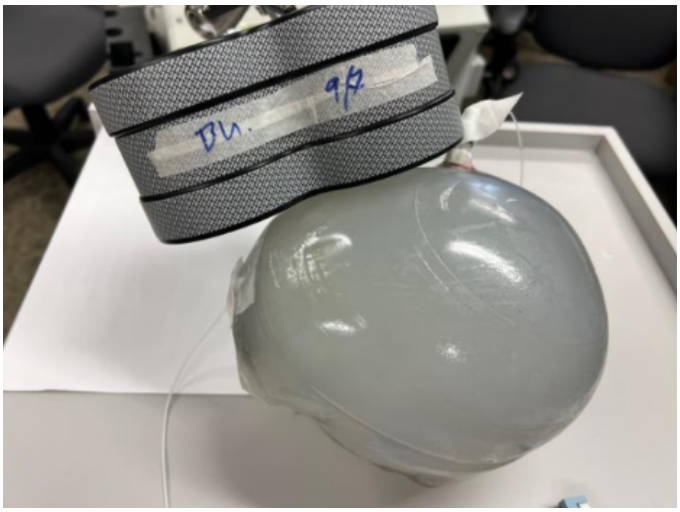

Figure 2: The adult brain phantom model developed at the University of Iowa [4].

The researchers on this project determined combined use was safe by analyzing the electrode change in temperature, displacement, and introduction of secondary electric currents. This study suggested the combined use of TMS and iEEG is safe for adults, which parallels the goals of this project; however, the safety of use in pediatric brains is the main priority, which has not previously been explored [4]. There are different physiological and electrical properties between the adult and pediatric brain, as well as different safety considerations. Because of this, the University of Iowa's gel phantom cannot be used to determine if TMS and iEEG are safe in pediatric patients. Pediatric brain phantoms do exist, but none meet the scope of this project. For example, there is a 3D-printed pediatric head phantom which accurately depicts the size and shape of a pediatric brain, but was fabricated to create an optimized protocol for pediatric computed tomography (CT) imaging. The brain of this phantom was made with epoxy resin, and the skull was made with plaster and resin [4]. As mentioned previously, the size and shape of the 3D-printed phantom matches this project, but there are no other similarities in their functionality.

Problem Statement

The goal of this project, therefore, is to develop a pediatric brain phantom model that can be used to simulate the main effects of TMS on iEEG electrodes – induced currents, temperatures, and changes in position – in order to verify that these brain mapping techniques can be used in tandem.

II. Background

As previously described, epilepsy is a complex neurological condition in which recurrent unprovoked seizures occur. These seizures are caused by short, excessive discharge of electrical activity in the brain: the abnormal propagation of electrical impulses can be caused by insufficient inhibition, excessive excitation, or a combination of both factors within the brain's neuronal network [1]. Various lobes within the cerebral cortex can be involved in seizure generation, each associated with differing symptoms or manifestations. There are several antiepileptic pharmacological treatments utilized in treating epilepsy, including both narrow-spectrum drugs that work for specific seizure types and broad-spectrum drugs that have some efficacy for a wider range of seizures. About 30% of patients have drug resistant epilepsy, however; in this case, another treatment option considered is that of surgical intervention. The mortality rate in children affected by epilepsy is 5 to 10 times higher than the rest of the population, so properly treating and controlling these unprovoked seizures is paramount [5].

The surgical approaches taken when pursuing epilepsy treatment can vary widely, depending on patient-specific pathology. As a whole, the techniques used prioritize minimal invasive procedures that still target epileptogenic zones. These zones are classified as the regions of the brain that are capable of generating seizures; upon removal or disconnection of these areas, seizure freedom can potentially be obtained [6]. Prior to undergoing operation, brain mapping techniques can generate spatial representations of the patient's brain to map out which regions are presenting abnormal behavior. One such method, iEEG, is routinely used in surgical planning and utilizes electrode systems that are either connected across the surface of or implanted into the brain. This method provides high spatiotemporal resolution and is especially advantageous for epileptogenic foci localization [7]. TMS, another technique, assesses brain circuit excitability through electromagnetic induction, inducing currents to produce action potentials and painlessly activate brain networks [8]. TMS is renowned for its noninvasive nature, as well as its capability to illustrate brain connectivity; its mechanism is displayed in Figure 3.

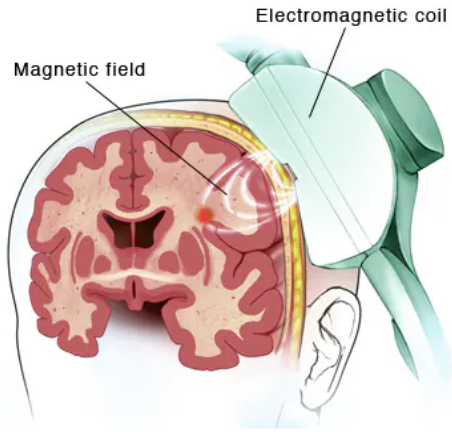

Figure 3: Application of a TMS coil to deliver a magnetic pulse [9].

As a result, both techniques may provide complementary information for mapping out critical brain regions that should be avoided during surgery. However, there are several safety concerns around the use of TMS in patients with iEEG: that of secondary electrical currents, heating of the implanted electrodes, and electrode array displacement, all of which would have severe consequences for the affected individuals [4]. Additionally, the impact of these techniques has only been studied on adult patients where dissimilar physiology and higher resting motor thresholds might require higher levels of stimulation during treatment compared to pediatric patients [10].

Client Information

The client for this project is Dr. Raheel Ahmed, a pediatric neurosurgeon at the American Family Children's Hospital (AFCH) who has a focus in pediatric epilepsy. The alternate contact for this project is Dr. Arun Manattu, a scientist at the Waisman Center's Pediatric Neuromodulation Laboratory (PNL).

Design Specifications

The phantom must accurately represent the physiology of an average pediatric brain and skull, with a skull circumference of 50-54 cm and overall volume of 1,300 cm^3 [11], [12]. The material chosen for the brain must have a similar electrical and thermal conductivity to brain tissue, approximately 0.2-0.5 S/m and 0.536 W/m-K, respectively [13], [14]. After TMS testing with the phantom is complete, the electrodes must express a less than 1 °C temperature, fewer than 30 $\mu C/cm^2$ difference in charge density, and minimal displacement. The phantom must comply with MTR Standards 2.4 and 3.3, CFR Standards 882.5802, and ASTM F2182, all describing safe practices for the use of iEEG or TMS [15], [16], [17]. The budget for this project is $500. See Appendix A for full design specifications.

III. Preliminary Designs

Hydrogel Material

Gelatin

Gelatin is a natural protein that is derived from the hydrolysis of collagen. Gelatin is widely used as a hydrogel due to its biodegradability, accessibility, and low cost. Its gelation is thermo-reversible at approximately 20-25 °C [18]. Gelatin's preparation includes polymerization, crosslinking, and hydrolysis. Adjusting the concentration or crosslinking of gelatin during its preparation can change the properties of the hydrogel like porosity, stiffness, and degradation rate [19].

Poly(acrylic acid) (PAA)

PAA is a synthetic polymer derived from the polymerization of acrylic acid. Despite being synthetic, PAA still shares many of the positive characteristics of natural hydrogels, such as being biodegradable, nontoxic, and biocompatible. As a synthetic material, PAA can be easily tuned to increase its mechanical properties via crosslinking or copolymerization [20].

Agar

Agar is a polysaccharide derived from the cell walls of seaweed. Agar is widely used in biomedical applications due to its biocompatibility and strong ability to gel. Agar is composed of a blend of agarose and agarose pectin, in which the agarose component allows for gelling. Gelation is thermoreversible and occurs slightly above body temperature. The mechanical properties of agar are generally considered to be low, but can be tuned by changing the concentration of agar, crosslinking, or incorporating other materials [21].

Agarose

Agarose is a polysaccharide derived from red algae or seaweed and is a purified form of agar. Agarose exhibits good biocompatibility, biodegradability, and thermoreversible gelling making it widely used in biomedical applications. Chemical or physical modifications allow agarose to be versatile and used in many different environments. The gelation of agarose occurs below or around body temperature, and this process is thermoreversible. Agarose on its own is considered brittle, but enzymatic modifications can improve this property. Processes like crosslinking can be used to tune agarose to the desired mechanical properties [22].

Skull Material

Poly(lactic acid) (PLA)

PLA is a thermoplastic polymer widely used in engineering and biomedical applications due to its biodegradable, biocompatible, and nontoxic properties. PLA is often derived from renewable materials such as corn starch and sugarcane and is most commonly used for rapid prototyping via 3D printing due to its wide accessibility and low cost [23]. While PLA has many advantages, it is considered disadvantageous due to its brittleness, low toughness, and slow crystallization rate [24]. The elastic modulus of PLA is 3.5 GPa and its tensile strength is 50 MPa [25].

Poly(methyl methacrylate) (PMMA)

PMMA is a thermoplastic polymer widely used in resin 3D printing which has a wide variety of possible molecular weights. Using different molecular weights of PMMA can change properties such as viscosity, elastic modulus, and brittleness. PMMA is considered advantageous due to its transparency and high strength. The elastic modulus of PMMA is between 18 and 31 GPa [26].

FormLabs BioMed Clear Resin (FBC)

FBC resin is a material commonly used for biomedical applications where there is long-term contact with the skin or mucosal membrane due to its biocompatibility. FBC resin is printed by FormLabs stereolithography (SLA) printers and may have a clear finish. FBC resin is compatible with common sterilization methods, including autoclaving and ethylene oxide sterilization, which make FBC versatile for many different applications. The elastic modulus of FBC resin is 2.08 GPa and its tensile strength is 52 MPa [27].

FormLabs Standard Resin (FS)

FS resin is a material that is commonly used for creating parts that require showcasing internal features, like fluidic devices, due to its highly transparent nature. FS resin is printed by a FormLabs SLA printer, capable of a quick printing speed while maintaining accuracy. The tensile strength of FS resin is between 46 and 60 MPa [28].

IV. Preliminary Design Evaluation

Design Matrices and Summary

Table 1: Hydrogel Material

Design Criteria	Weight	Gelatin		Poly(acrylic acid)		Agar		Agarose	
Thermal Conductivity	20	2/5	8	3/5	12	5/5	20	1/5	4
Preparation	20	2/5	8	4/5	12	5/5	20	4/5	16
Tunability	20	1/5	5	5/5	20	3/5	12	3/5	12
Reactivity	15	4/5	12	3/5	9	2/5	6	3/5	9
Shelf Life	15	1/5	3	4/5	12	3/5	9	3/5	12
Cost	10	5/5	10	2/5	4	4/5	8	2/5	4
Total	100	46		69		75		57	

Thermal Conductivity

The thermal conductivity criteria analyzes how easily a material conducts heat. A high thermal conductivity value indicates the material is a great conductor and readily passes heat. The brain has a thermal conductivity of 0.536 W/m-K, and the chosen material should be within a similar range [14]. Agar was a close match to the thermal conductivity of the brain, measuring 0.52 W/m-K [29]. PAA and gelatin were slightly less than this at 0.37 and 0.30 W/m-K, respectively [30], [31]. The thermal conductivity of agarose was significantly less than the brain, only offering conductivity of 0.121 W/m-K [32].

Preparation

Preparation is defined as the level of difficulty that is required to prepare the hydrogel, as well as the methods of fabrication possible for each material and their compatibility with this project. Factors like time and amount of materials needed are considered in the difficulty of preparation. The hydrogel that requires the least amount of time and materials will score the highest. An ideal hydrogel will also be able to take on an anthropomorphic brain shape, most easily achieved via a photoactivation fabrication technique [33]. Of the reviewed materials, gelatin is the only that requires chemical modification in order to remain stable at room temperature, despite having a relatively simple preparation without these modifications [18]. The required modifications gelatin the lowest score in this category, while agar's simple gelation and greater stability at room temperature gave it the highest score. Agarose and PAA scored intermediately as they both require other materials and multiple steps to prepare.

Tunability

Tunability refers to the ability to adjust various material properties of the hydrogel via changes in its concentration, crosslinking, and other techniques. Material properties are crucial in determining which gel is most similar to the average pediatric brain, but these can differ significantly based on adjustments made to the gel. The gel that scores the highest will be the gel with the best tunability. In general, synthetic polymers are more easily tunable than natural polymers, as they are more controlled and consistent [34]. Because of this, PAA scored the highest as it is the only synthetic material. Gelatin scored the lowest as it is not tunable on its own and requires chemical modifications to become easily tunable [35]. Agar and agarose scored in the middle, as they can be easily modified by changing their concentrations, but are less precise than PAA due to being natural materials.

Reactivity

Reactivity refers to the hydrogel toxicity levels, compatibility with the skull polymer, and durability throughout each testing period. The hydrogel should pose no significant harm to the handler when performing safe care with the gel such as wearing gloves and avoiding ingestion. The hydrogel also must not induce a reaction of any sort with the exterior skull mold that will encase the internal brain phantom. Lastly, the material must be able to maintain its structure throughout a single testing period with iEEG and TMS, ensuring little variation in results due to external sources. Agar scored the lowest due to its toxicity when inhaled and in contact with the skin [36]. Additionally, it does not maintain its structure as well as the other gels when needle-like items are inserted into the material [37]. PAA scored in the middle because although it is generally non-toxic, it also does not maintain its structure after having items inserted into it [38], [39]. Agarose earned the same score as PAA because although it can recover from item insertion, it has higher toxicity levels [40], [41]. Gelatin was rated the highest because it is non-toxic and will maintain its structural integrity [42], [43]. None of the materials are expected to react with the cured resin material that will be used for the 3D-printed skull.

Shelf Life

Shelf life is defined as the gel's degradability rate or time before the gel must be replaced during testing. The hydrogel with the slowest degradability rate and longest amount of time before it needs replacement will score the highest, as this gel is the most efficient to use. The gel that scored the lowest was gelatin due to its thermal instability and quick degradation rate [44]. PAA scored the highest as it is a synthetic polymer that is not subject to enzymatic or hydrolytic degradation [45]. Agar and agarose scored intermediately, with degradation rates of weeks to months [46], [47].

Cost

The cost criteria is the price of each hydrogel per gram. Gelatin is the least expensive material by far, costing $0.05 per gram [48]. Agar had the next best price being approximately $0.39 per gram [49]. Lastly, agarose and PAA were given the same ranking, costing $1.51 and $1.74 per gram, respectively [50], [51].

Table 2: Skull Material

Design Criteria	Weight	Poly(lactic acid) (PLA)		Poly(methyl methacrylate) (PMMA)		FormLabs BioMed Clear		FormLabs Standard Resin	
Reactivity and Shelf Life	25	3/5	15	5/5	25	4/5	20	3/5	15
Transparency	20	1/5	4	5/5	20	5/5	20	3/5	12
Permittivity	20	2/5	8	3/5	12	5/5	20	5/5	20
Accessibility	15	5/5	15	1/5	3	4/5	12	4/5	12
Mechanical Properties	10	2/5	4	5/5	10	5/5	10	3/5	6
Cost	10	5/5	10	1/5	2	3/5	6	4/5	8
Total	100	56		72		88		73	

Reactivity/Shelf Life

Reactivity is defined as the relative likelihood of the skull polymer to react with, including enhance the degradation of, the brain phantom hydrogel. Both FormLabs filaments are described as non-reactive under recommended conditions, and have very high boiling and flash points. Shelf life refers to the polymers rate of degradation, especially when exposed to water. This is primarily relevant to prevent rapid degradation of both the skull material and the subsequent changes to the properties of the hydrogel material caused by reactions with any dissolved skull materials. PMMA, followed by PLA and FBC display the slowest rate of degradation in water. In this category, however, FBC scored highest due to extensive safety and degradation testing with positive results. It is important to note that the reactivity of each skull polymer will depend on the chosen brain hydrogel material – crosslinking agents such as peroxides should be avoided [27].

Transparency

The transparency category describes the need for optical clarity with regards to the brain phantom itself. One of the main focuses of the client is to measure possible displacement of implanted and surface electrodes during the application of TMS current; in order to capture this potential movement, the user must be able to visualize the phantom itself. In a similar recent study, clarity was essential, as a motion capture camera system was used to measure said displacement. As such, two material options scored the highest in this category: PMMA and FBC resin. Both materials are suitably clear, as PMMA is often touted as a glass substitute and FBC resin is recommended for visibility purposes [27], [52].

Permittivity

Permittivity refers to a material's ability to allow electric field generation across it. In the context of this project, permittivity closest to that of cranial bone is preferred: around 2.76×10^2 F/m in the case of cancellous bone, and around 1.53×10^2 F/m in the case of cortical bone [53]. This value is crucial for accurate testing values and ensuring patient safety. All four polymers displayed similar lower permittivities when compared to cranial bone. PMMA and PLA reported values of 2.76 and 2.5 F/m, respectively, at maximum while FormLabs resin options displayed comparatively higher permittivity values, in the range of 3-4 F/m [54], [55]. Thus, these two materials were deemed closest to physiological, relative permittivities. It is important to consider these differences between physiological and polymeric permittivity when establishing testing procedures.

Accessibility

PMMA was by far the least accessible, due to the fact that it is not stocked as a material option in the University of Wisconsin-Madison's Grainger Design and Innovation Lab at Wendt Commons (DI Lab), leading to the need to outsource a 3D printing service. Options for this would be to submit prints to a fee for printing service, but these prints have a long lead time and no direct control over the printing process. Another option would be to purchase a spool of PMMA filament, requiring access to a printer not at the DI Lab. In contrast PLA, FBC resin, and FS resin are all available to print in the DI Lab. PLA is the most accessible, as it is available on the greatest number of printers and requires no post-processing once the print is complete. Both FormLabs resins are slightly less accessible due to the fact that there are less available FormLabs printers, and require DI Lab staff to perform post-processing to cure the final print to the desired finish.

Mechanical Properties

The mechanical properties of the skull material were deemed necessary to consider as well. Although the skull is not under mechanical duress during TMS testing, meaning that tensile or elastic moduli were of little consequence to the material choice, finding a material with

appropriate porosity to provide similar supportive capabilities to the human skull was preferable. Once again, both PMMA and the FBC resin were rated the highest in this category. The mean reported elastic modulus for the human skull is around 8.51 GPa; resin has been found to have an elastic modulus of around 2.8 GPa, while acrylic-based polymers reportedly present elastic moduli around 2.15 GPa. As both of these values are on the same magnitude of relevant human skull properties, both materials received high scores [56]. Porosity was also considered, given the reported porousness of human bone. However, this was not factored as heavily into this rating given the inherent capability of 3D-printed parts to achieve a porous structure using a variety of materials [57].

Cost

Cost was defined as the cost to 3D print the materials per gram. PLA was by far the most affordable, at $0.05 per gram. FS resin is the next most affordable at $0.24 per gram and FBC resin is priced at $0.42 per gram [23]. While the direct cost of PMMA is typically around $0.07 per gram, due to a lack of accessibility, there is an upfront cost associated with using this material. One option is the prints would have to be outsourced to a third party 3D printing service, 3ERP, which quoted $27 per gram to print in PMMA [58]. Another option is purchasing an entire spool of PMMA filament costing in the range of $50-$67 for one kilogram [59].

Proposed Final Design

The proposed final design is a head phantom that accurately mimics the size and shape of a pediatric head, similar to the design shown in Figure 5. The brain of the phantom will be created using an agar hydrogel that incorporates a sodium chloride (NaCl) solution to increase its electrical conductivity to match that of brain tissue. The skull of the phantom will be 3D printed with FBC resin.

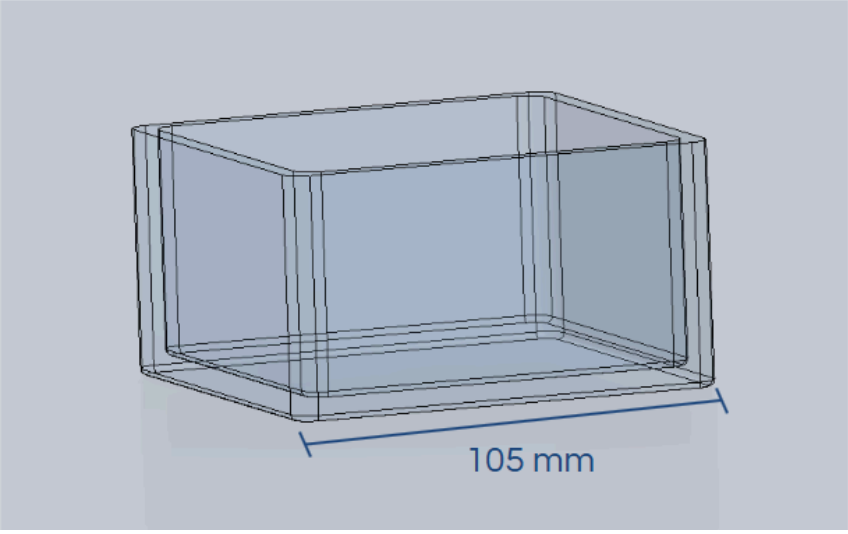

Figure 4: Pediatric sized gel box phantom CAD model.

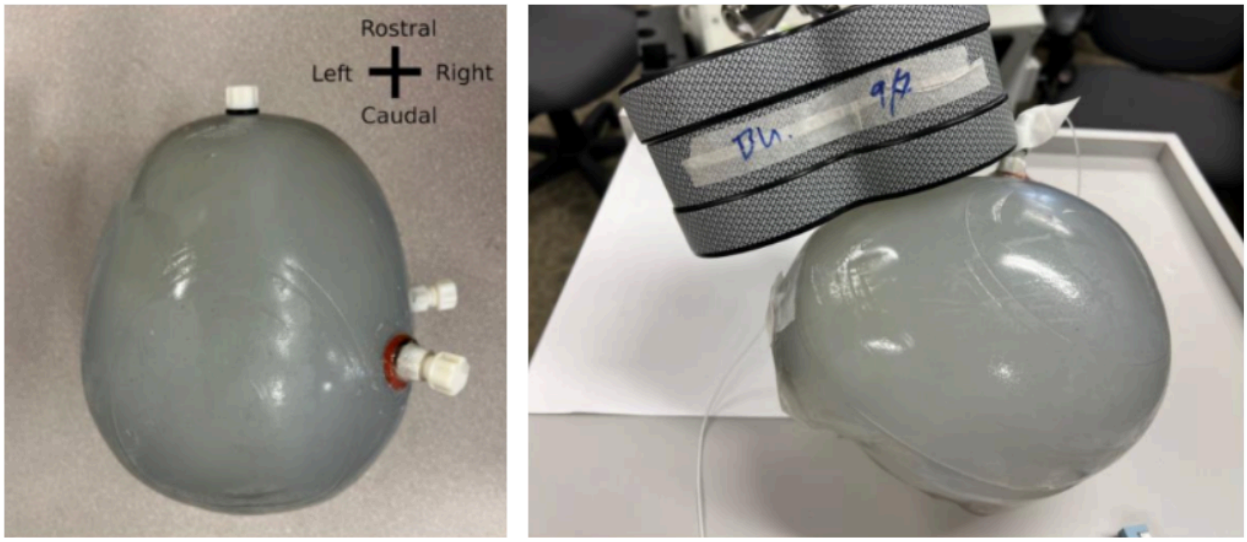

Figure 5: University of Iowa skull-based phantom, to be adapted to pediatric size [4].

V. Fabrication

Materials

Skull Base:

FBC resin was chosen as the material for the skull base. FBC is an acrylate, urethanedimethacrylate, methacrylate copolymer with a Young's Modulus of 2.08 GPa [27] consistent to an order of magnitude with the stiffness of cranial bone [56]. Additionally, this material is readily available to 3D print at the DI Lab at the price of $0.24 per gram [57].

Brain Tissue

The brain tissue material will consist of a natural polymer tuned with NaCl for electrical conductivity [60]. At present, both gelatin type A and agar are being considered for the polymer. Head-to-head testing will be completed next semester to directly compare the options. Gelatin Type A was purchased at 100 g from MilliPore Sigma at a price of $0.54 per gram [61]. Agar powder was purchased at 500 g from ThermoFisher Scientific for $0.26 per gram [49].

Gelatin

Gelatin is a denatured form of collagen, a ubiquitous protein in animal tissue. Gelatin forms a thermoreversible gel around 20 ℃ and melts quickly around 35 ℃. Gelatin hydrogels form by physical entanglements of triple helices, which is illustrated in Figure 6. Gelatin forms a homogenous, ordered gel, making mechanical characterization straightforward. However, it has a tendency to slowly degrade at room temperature.

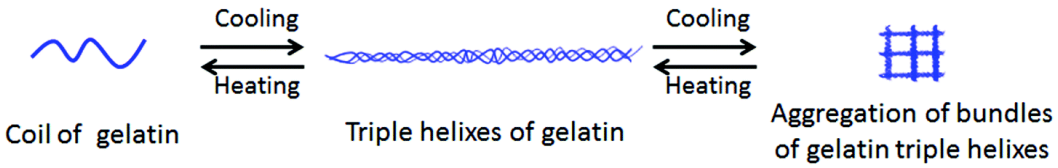

Figure 6: Microstructure of gelatin hydrogel [62].

Agar

Agar is a derivative of seaweed sugars, made of a combination of polysaccharides agarose and agarose-lectin [21]. Agar gels at room temperature (25 ℃) by physical entanglement of sugar coils or chemical crosslinking. Figure 7 shows how agar sugars form random coils that can make their microstructure non-homogenous upon cooling. Agar therefore offers improved thermal properties but introduces a layer of complexity when considering mechanical characterization.

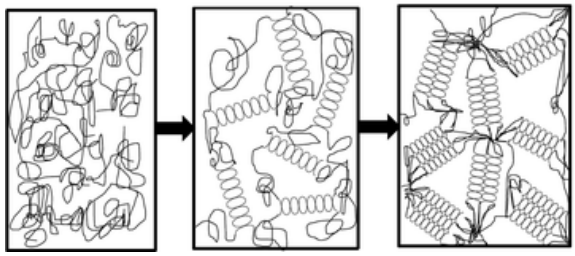

Figure 7: Microstructure of agar hydrogel [63].

Methods

Skull Base

An initial prototype of the brain tissue was fabricated in a PLA square mold, similar to the University of Iowa preliminary phantom in Figure 4 [4]. This box phantom was printed in PLA to carry out material testing on the gel itself.

CT scans of pediatric patients provided by the client were processed into 3D printable files using the pipeline seen in Figure 8. Briefly, Digital Imaging and Communications in Medicine (DICOM) files were uploaded to the 3D Slicer software, refined, and exported as standard triangle language (STL) files into SolidWorks (Figure 9). A detailed protocol can be found in Appendix B and C. Moving forward, MRI scans will be used to generate soft tissue printable molds using a similar processing pipeline. The base of these molds will be 3D printed in PLA, after which Ecoflex silicone will be used to create a soft, pliable mold where hydrogels can form, set, and be easily removed.

The final skull model will be 3D printed on a FormLabs stereolithography (SLA) printer. SLA 3D printing involves layer-by-layer deposition of liquid-phase resins, which are UV-cured as they are deposited [64].

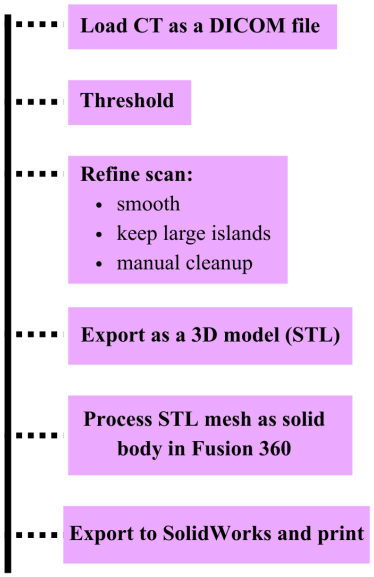

Figure 8: File processing pipeline for 3D printable skull.

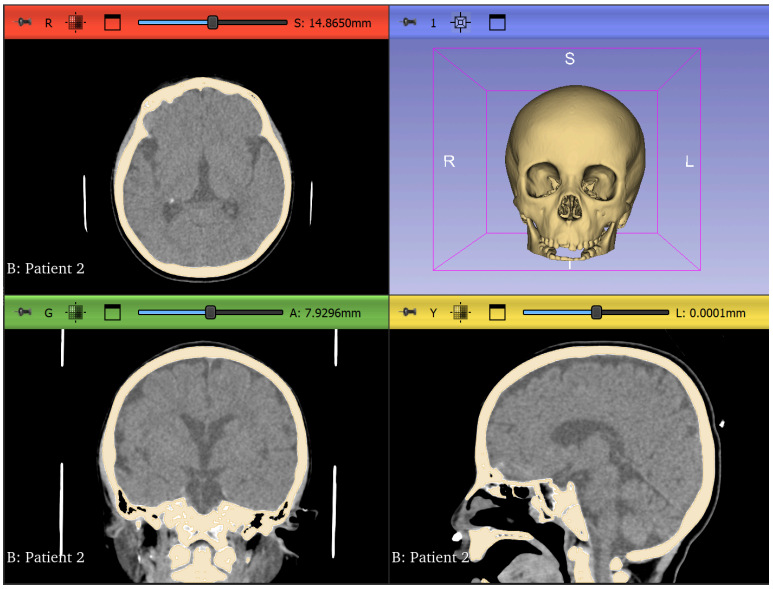

Figure 9: Segmenting CT scan of pediatric patient into skull model in 3D Slicer.

Brain Tissue

Both hydrogel material options follow the same fabrication protocol, which is summarized in Figure 10 below and detailed in Appendix D.

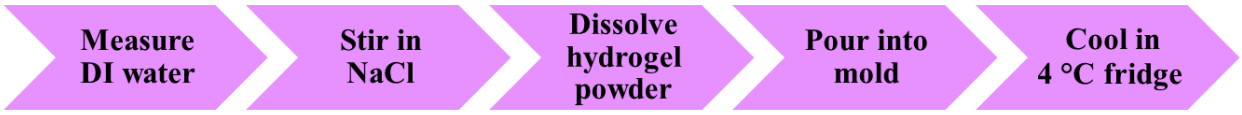

Figure 10: General hydrogel fabrication protocol.

Final Prototype

The final prototype of this project will be a brain and skull phantom, representing the anatomy of an average 5 to 7 year old pediatric cranium. The skull will be made of a clear resin 3D-printable photopolymer. The geometry of the skull will be obtained by processing CT scans provided by the client, as seen in Figure 11.

The brain tissue will be made up of either a gelatin or agar based hydrogel. A gelatin hydrogel would be composed of 6% Type 1 gelatin, while an agar hydrogel would be composed of 1.2% agar powder. Each of these hydrogels would be tuned with <1% NaCl, and the remaining volume would be composed of DI water.

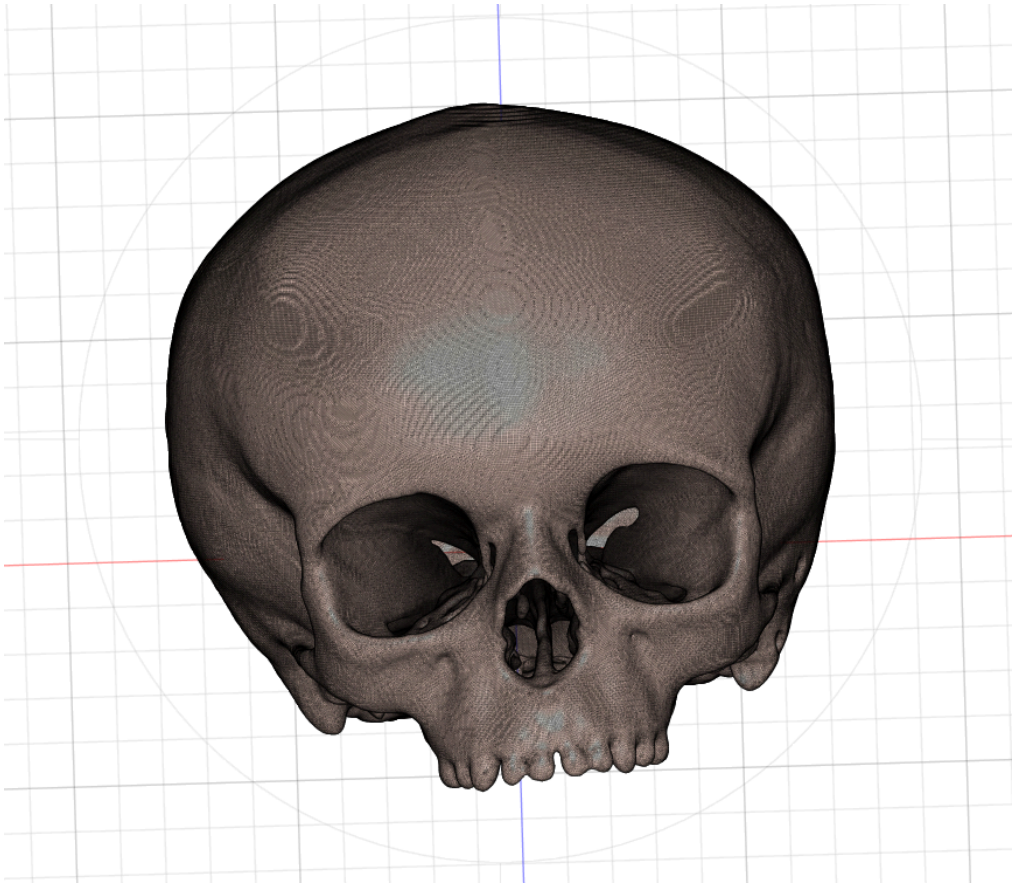

Figure 11: 3D CAD model of pediatric skull base from processed CT scans.

VI. Testing

Mechanical Properties

To classify mechanical characteristics of the chosen hydrogel, shrink-swell testing was performed (Figure 12). Analyzing material behavior in environments with varying solvents presents valuable information on hydrogel durability and the consistency of its mechanical properties. Because brain tissue characteristics stay relatively constant over short periods of time, the ideal hydrogel and corresponding concentration must exhibit small variations when exposed to solvents. In this case, 100% ethanol (EtOH) and deionized (DI) water were used to shrink and swell the materials, respectively. Testing was performed on 0.5%, 1.0%, and 1.5% agar, with 3 replicates for each concentration. The full testing protocol can be seen in Appendix E. The mass of each hydrogel is expected to decrease when placed in EtOH, but when returned to DI water, the structure must remain fully intact while not greatly exceeding the original recorded mass, ensuring similar structural integrity to that of brain tissue [65]. Gels with a higher water concentration were expected to vary the most, while gels with higher polymer concentrations are expected to vary the least. The statistical significance between conditions will be analyzed using a one-way ANOVA test within MATLAB, which is shown in Appendix F, as well as one-sample and paired t-tests. When deciding between agar and gelatin, the hydrogel with the most consistent trends across varying concentrations will be favored.

Figure 12: Shrink-swell testing with agar.

Thermal Properties

Thermal conductivity, or the heat transfer behavior of a material, is crucial for ensuring proper heat distribution during testing. To confirm that the final brain phantom iEEG and TMS testing is translatable to human patients, the phantom must closely match the thermal conductivity of pediatric brain tissue, approximately 0.536 W/m-K [14]. Testing was done on

gelatin samples of 4%, 6%, and 8% concentrations, using 3 replicates each. Temperature measurements were taken instantaneously over a 10 minute period using the circuit seen in Figures 13 and 14 below, which features an LT1025 cold junction, K-type thermocouple, and low-pass filter. Temperature values were recorded and reported using an Arduino Uno and the corresponding Arduino IDE software. The code used for this process is shown in Appendix G. The general procedural setup is illustrated in Figure 15, where the thermocouple was inserted into a rectangular hydrogel sample at a known depth as it heats on a 35 °C hot plate. The change in temperature was then used in (1) to determine thermal conductivity, k (W/m-K), where m is mass (kg), c is specific heat capacity (J/kg-K), $\frac{dT}{dt}$ is the rate of temperature change (K/s), Δx is separation (m), A is surface area (m^2), and ΔT is the temperature difference (K). The MATLAB script in Appendix H was used to perform calculations and run statistical analyses via a one-way ANOVA. The hydrogel type and concentration most similar to the defined goal value will be chosen. The full testing protocol can be found in Appendix I.

$$k = \frac{m*c*\frac{dT}{dt}*\Delta x}{A*\Delta T} \quad (1)$$

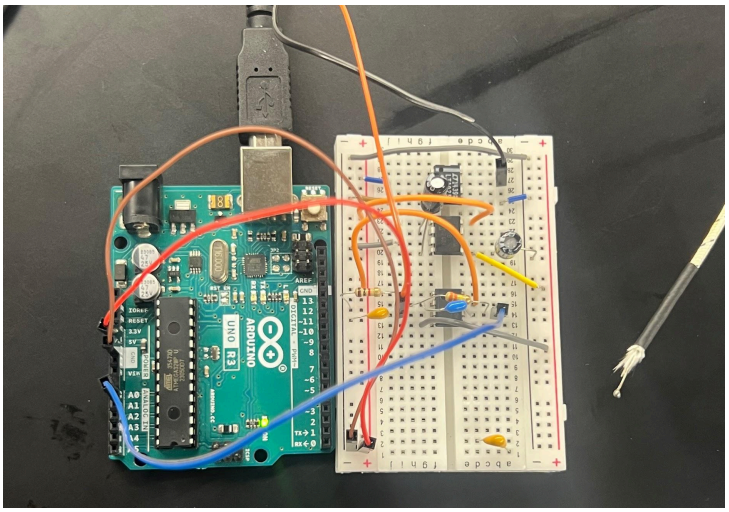

Figure 13: Thermocouple circuit.

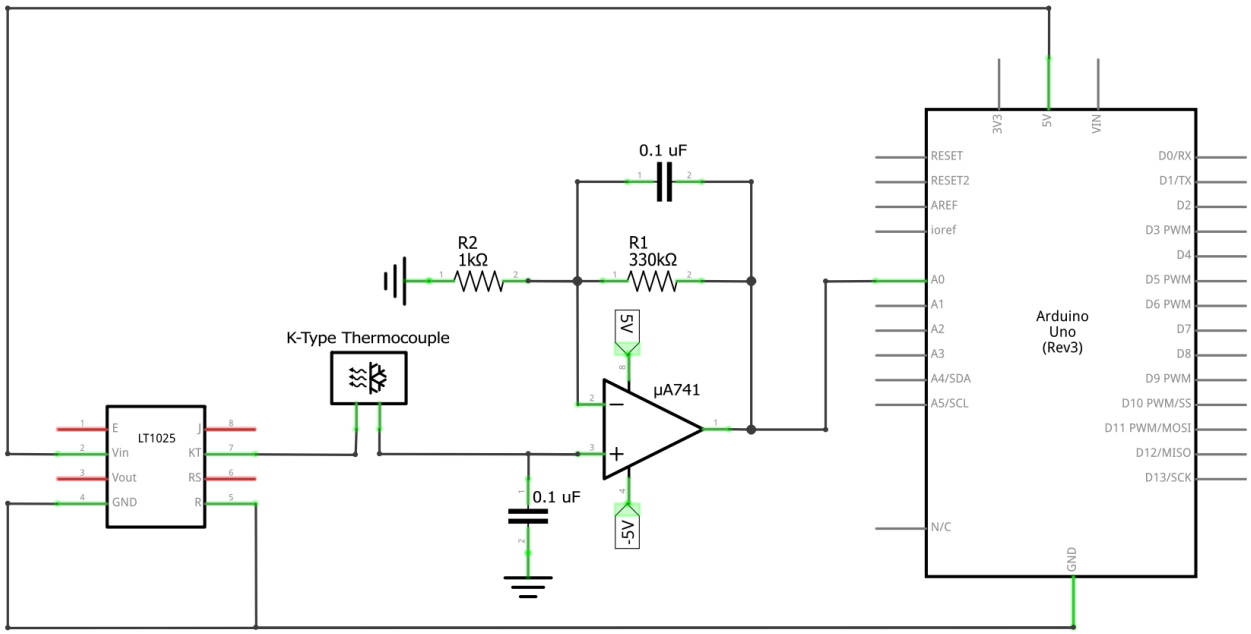

Figure 14: Thermocouple schematic.

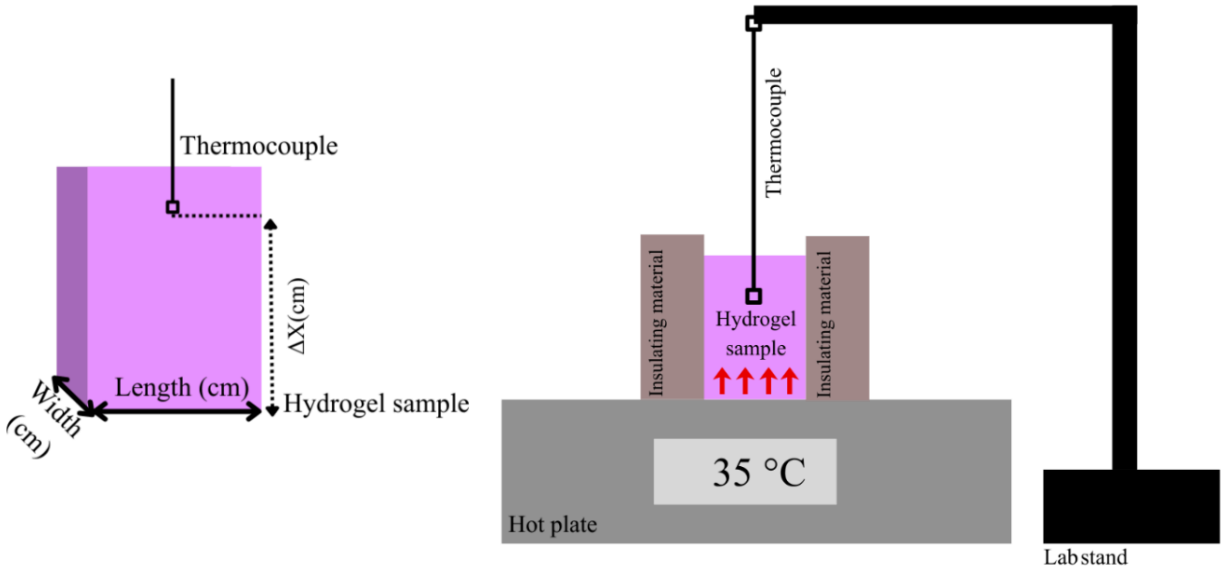

Figure 15: Thermal conductivity testing setup.

Future Testing

In order to further characterize both the agar and gelatin hydrogels and their fine-tuned derivatives, additional material testing is planned for next semester. Ultimately, either agar or gelatin will be selected based on which can best balance thermal conductivity, electrical conductivity, and relative mechanical strength compared to pediatric brain tissue. Specifically,

the testing protocols described above will be repeated for both agar and gelatin in addition to electrical conductivity testing and mechanical characterization via a rheometer.

The final testing procedure for mechanical properties will be adapted from the Franck lab at UW-Madison, which uses Inertial Microcavitation Rheometry (IMR) to find hydrogel shear modulus values [66]. For determining the electrical conductivity of each material, a current will be generated across each respective hydrogel sample, where the voltage drop can then be measured and further used to calculate electrical conductivity. Equations (2), (3), and (4) shown below represent the full mathematical process to find electrical conductivity, σ (S/m), where V is the voltage drop (V), I is induced current (A), R is resistance (Ω), ϱ is resistivity (Ω-m), A is surface area (m^2), and L is length (m). A full planned testing protocol can be found in Appendix J.

$$V = IR \tag{2}$$

$$\rho = \frac{R*A}{L} \tag{3}$$

$$\sigma = \frac{1}{\rho} \tag{4}$$

VII. Results

Mechanical Properties

The results of shrink-swell testing with agar are shown graphically in Figure 16. As a general trend, each sample decreased in mass most during the first 20 minutes. Little variation was observed in the remaining 40 minutes, however, 1.0% agar maintained a fixed mass more readily than the other concentrations. The average percent decrease of 0.5%, 1.0%, and 1.5% groups was 30.3 ± 15.9, 25.3 ± 2.46, and 23.9 ± 3.14, respectively. As expected, lower concentrations of agar were associated with a greater decrease in mass. The 0.5% group, however, exhibited a large standard deviation, suggesting possible human error during fabrication of the samples.

To compare initial versus final mass within conditions, paired t-tests were done across the whole data set of each condition. These tests were carried out in order to validate the testing protocol and shrinking trends across gels in the same group. The paired t-tests revealed p-values of 0.07, 0.005, and 0.01 for the 0.5%, 1.0%, and 1.5% agar conditions respectively. These results indicate that the 0.5% agar gel did not have significant shrinkage, while the 1% and 1.5% agar gels did, contrary to the expected results and trends suggested by the average percent decrease.

Additionally, a one-way ANOVA analyzing the shrinking behavior between each concentration returned a p-value of 0.4176, signifying no significant difference between groups. After shrinking, the samples were returned to water, which resulted in increased mass compared to the initial measurements. Specifically, 0.5% agar experienced a percent increase of 13.3 ±

4.08, 1.0% had 20.2 ± 2.78, and 1.5% had 13.8 ± 1.4. ANOVA analysis revealed a p-value of 0.0828, once again suggesting no significant difference across groups from this round of testing. Each concentration experienced greater swelling than is ideal, however, the integrity of each sample was maintained despite the noticeable increase in mass.

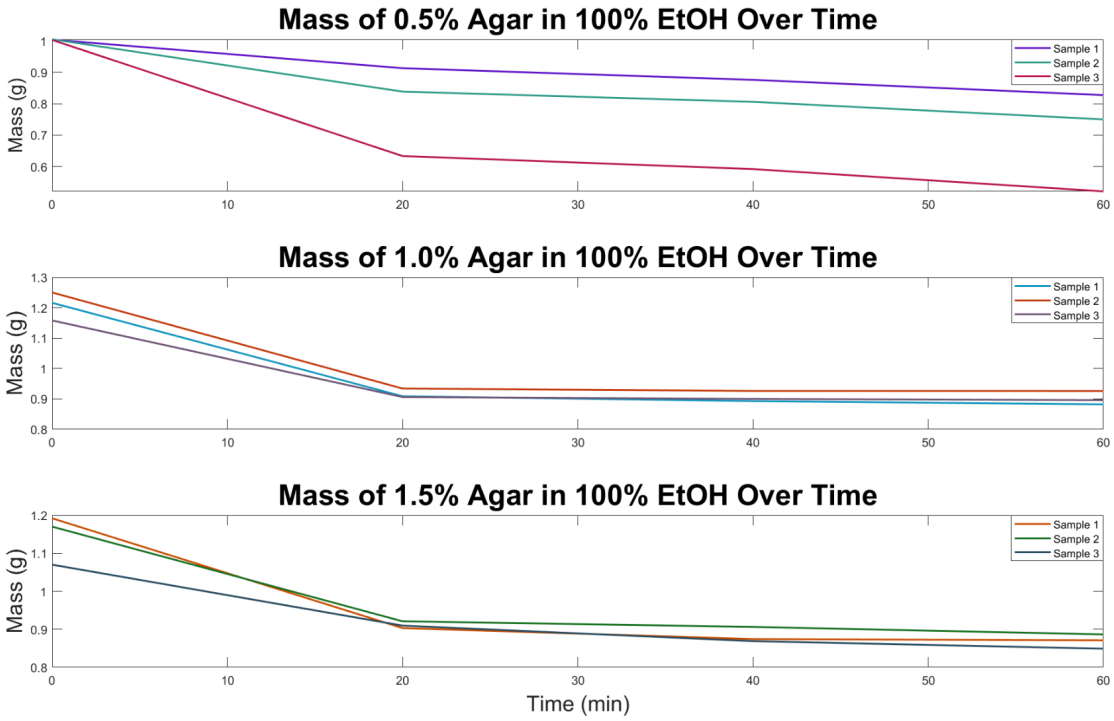

Figure 16: Agar behavior over time when submerged in 100% EtOH.

Thermal Properties

Results from taking thermal conductivity measurements with gelatin samples are represented in Figure 17. The calculated values for 4%, 6%, and 8% gelatin are 0.32 ± 0.07, 0.67 ± 0.23, and 0.47 ± 0.09 W/m-K, respectively. There is no significant trend expressed in these results to relate gelatin concentration to the corresponding thermal conductivity value, as the current outcome suggests 6% gelatin has the highest thermal conductivity of the three. The 6% samples, however, expressed an unusually high standard deviation, so testing will be repeated to ideally reveal more reliable results. Presently, 8% gelatin most closely resembles pediatric brain tissue, with only a 13.1% difference compared to 42.9% and 26.6% in the 4% and 6% groups. One-way ANOVA analysis gave a p-value of 0.082, again showing no significant difference between sample groups. The concentration of NaCl was held fixed in each sample, which may be contributing to the unexpected results. In the future, experimentation with concentration of saline solutions in each hydrogel may reveal more accurate results that better resemble expected thermal conductivity in brain tissue.

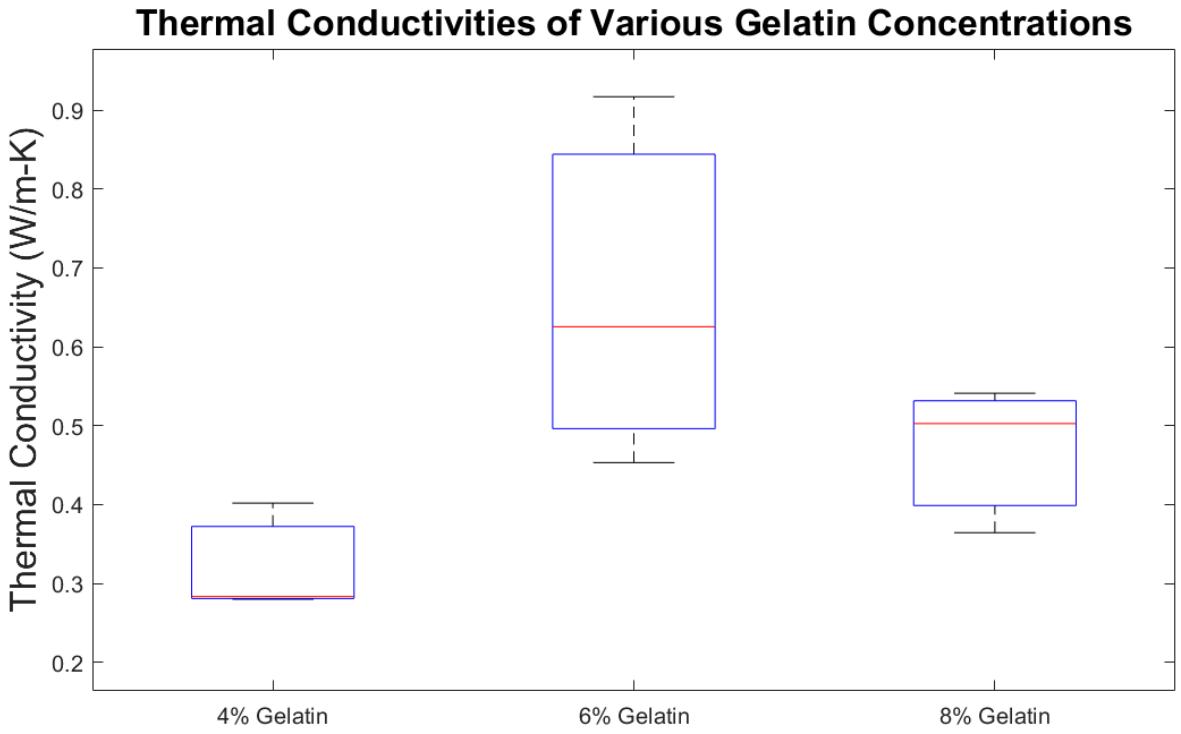

Figure 17: Thermal conductivity of gelatin with varying concentrations.

VIII. Discussion

Completion of this phantom will allow Dr. Ahmed and his team to validate the use of TMS in conjunction with iEEG for pediatric patients. A recent study conducted at the University of Iowa experimented with the combined use of TMS with iEEG on adult patients [4]. Initial testing was performed using a gel box phantom, followed by a skull-based phantom. While this addressed several of the current project's concerns, it failed to consider more stringent safety standards and physiological differences present in pediatric patients.

Due to pediatric involvement, this project requires particular ethical considerations. iEEG is currently approved for use in pediatric patients and is routinely used in surgical planning for patients with uncontrolled seizures. However, while there have been several studies investigating the use of TMS, there is still a lack of formal guidelines or standard protocols for pediatric patients. As a research tool, this phantom must accurately represent a pediatric brain in electrical and mechanical aspects in order to collect results on the efficacy of TMS used with iEEG. Responsible conduct of research and development standards must be upheld. A risk analysis should also be performed to mitigate potential sources of error. If the final phantom fails in any of the three testing scenarios of electrode displacement, heating, or current generation, the researchers should not proceed with in-vivo testing on pediatric subjects.

For each of the three ANOVA tests performed across testing conditions, there was insufficient evidence to reject the null hypothesis. Although the main objective for hydrogel

characterization is to match its properties to that of pediatric brain tissue, it is still important that a significant difference between sample groups is observed. This ensures if future concentration changes need to be made, the modifications in material properties are predictable. The non-monotonic behavior for thermal conductivity, which was shown graphically and through statistical inspection, suggests testing must be repeated. Some sources of error include inconsistencies with sample sizes, purity issues from using food-grade gelatin, or poor sample handling prior to testing. To minimize error when retesting, samples will be cut into rectangles of equal dimensions, and the thermocouple will be inserted at the same depth for each gel. Additionally, samples must only be removed from the 4 ℃ fridge immediately before the 10 minute testing period begins, helping to eliminate temperature variability.

The results from shrink-swell testing followed a more predictable trend. However, ANOVA statistical analyses and high standard deviations, especially within the 0.5% agar group, revealed retesting is needed. Paired t-test revealed that the 1.0% and 1.5% agar gels shrunk a statistically significant amount across the 60 minute testing window, while there was not sufficient mass loss in the 0.5% agar gel to reject the null hypothesis. These results indicate inconsistencies in either testing or gel preparation for this particular condition, as a significant amount of mass loss was expected for the lowest percentage agar gel. This inconsistency was further confirmed with the high standard deviation in this dataset.

A potential human source of error within shrink-swell testing may be from the 20, 40, and 60 minute time-points being relative, as each sample could not be weighed at the exact increments defined. Another factor contributing to unexpected results could arise from the inconsistent curing behavior of agar gels. Further, comprehensive characterization of agar's mechanical properties is often complicated by the tendency of its final microstructure to present as randomly formed coils. By following strict fabrication and testing procedures which require close attention to timeliness and proper documentation, these sources of error could be greatly suppressed.

IX. Conclusions

Epilepsy is the fourth most common neurological disease, often manifesting in pediatric patients before the age of one year [1]. iEEG is routinely used in surgical planning for epilepsy in adult and pediatric patients, and TMS may provide complimentary information for mapping critical regions of the brain that should be avoided during surgery. However, there are still many safety concerns around the use of TMS in patients with iEEG electrodes actively implanted. This project aims to develop a phantom for validation of use of TMS in pediatric patients with implanted cortical electrodes.

The complicated microstructure of agar makes it difficult to tune the exact mechanical properties needed and test using a rheometer. Additionally, the agar hydrogels were prone to contamination and allowed microbial growth during storage. Gelatin is not as stable at room temperature compared to agar and requires storage in a 4 ℃ refrigerator between testing

sessions. However, the preference for gelatin over agar in the Franck Lab, which focuses on traumatic brain injury research, makes a compelling case for its use and would provide a plethora of fabrication and testing methods to reference. Additionally, the electrical conductivities of both agar and gelatin can likely be varied based on the concentration of NaCl added, instead of relying solely on hydrogel concentration. Further testing is needed to confirm this hypothesis.

Moving forward, gelatin and agar will be tested head-to-head for thermal, electrical, and mechanical properties using the protocols described previously. While gelatin is more readily characterized mechanically compared to agar, there are potential benefits from both which are worth exploring. In addition to future characterization, two hydrogel brains will be made with implanted electrodes, one 6% gelatin and one 1.2% agar. The brains will be formed from a silicone mold which replicates a provided MRI scan. The final brain will be placed in a 3D-printed skull which will be fabricated in two sections, allowing the brain to be easily removed and replaced. The final goal for the project is to complete TMS testing on the phantom with both hydrogels in order to make a final recommendation on which gel to use for further testing.

References

[1] T. A. Milligan, “Epilepsy: A Clinical Overview,” *Am. J. Med.*, vol. 134, no. 7, pp. 840–847, July 2021, doi: 10.1016/j.amjmed.2021.01.038.

[2] G. Askari, M. Vajdi, S. Jafari-Nasab, and S. Golpour-Hamedani, “Ethical guidelines for human research on children and adolescents: A narrative review study,” *J. Res. Med. Sci. Off. J. Isfahan Univ. Med. Sci.*, vol. 29, p. 53, Aug. 2024, doi: 10.4103/jrms.jrms_610_23.

[3] K. Parkar, “National Epilepsy Week 2023,” The Voice for Epilepsy. Accessed: Dec. 10, 2025. [Online]. Available: https://thevoiceforepilepsy.co.uk/national-epilepsy-week/

[4] J. B. Wang *et al.*, “Effects of transcranial magnetic stimulation on the human brain recorded with intracranial electrocorticography,” *Mol. Psychiatry*, vol. 29, no. 5, pp. 1228–1240, May 2024, doi: 10.1038/s41380-024-02405-y.

[5] C. Minardi *et al.*, “Epilepsy in Children: From Diagnosis to Treatment with Focus on Emergency,” *J. Clin. Med.*, vol. 8, no. 1, p. 39, Jan. 2019, doi: 10.3390/jcm8010039.

[6] F. Winter *et al.*, “Current state of the art of traditional and minimal invasive epilepsy surgery approaches,” *Brain Spine*, vol. 4, p. 102755, Jan. 2024, doi: 10.1016/j.bas.2024.102755.

[7] Y. Wang, J. Yan, J. Wen, T. Yu, and X. Li, “An Intracranial Electroencephalography (iEEG) Brain Function Mapping Tool with an Application to Epilepsy Surgery Evaluation,” *Front. Neuroinformatics*, vol. 10, p. 15, Apr. 2016, doi: 10.3389/fninf.2016.00015.

[8] J.-P. Lefaucheur, “Chapter 37 - Transcranial magnetic stimulation,” in *Handbook of Clinical Neurology*, vol. 160, K. H. Levin and P. Chauvel, Eds., in Clinical Neurophysiology: Basis and Technical Aspects, vol. 160. , Elsevier, 2019, pp. 559–580. doi: 10.1016/B978-0-444-64032-1.00037-0.

[9] “Transcranial magnetic stimulation - Mayo Clinic.” Accessed: Dec. 10, 2025. [Online]. Available: https://www.mayoclinic.org/tests-procedures/transcranial-magnetic-stimulation/about/pac-20384625

[10] E. N. Sutter, C. P. Casey, and B. T. Gillick, “Single-pulse transcranial magnetic stimulation for assessment of motor development in infants with early brain injury,” *Expert Rev. Med. Devices*, vol. 21, no. 3, pp. 179–186, Mar. 2024, doi: 10.1080/17434440.2023.2299310.

[11] “Head circumference for age.” Accessed: Sept. 13, 2025. [Online]. Available: https://www.who.int/tools/child-growth-standards/standards/head-circumference-for-age

[12] E. Lüders, H. Steinmetz, and L. Jäncke, “Brain size and grey matter volume in the healthy human brain,” *NeuroReport*, vol. 13, no. 17, p. 2371, Dec. 2002.

[13] G. Halnes, T. V. Ness, S. Næss, E. Hagen, K. H. Pettersen, and G. T. Einevoll, *Electric Brain Signals: Foundations and Applications of Biophysical Modeling*, 1st ed. Cambridge University Press, 2024. doi: 10.1017/9781009039826.

[14] A. Mohammadi *et al.*, “Measurement of Ex Vivo Liver, Brain and Pancreas Thermal Properties as Function of Temperature,” *Sensors*, vol. 21, no. 12, June 2021, doi: 10.3390/s21124236.

[15] T. N. Tsuchida *et al.*, “American Clinical Neurophysiology Society Standardized EEG Terminology and Categorization for the Description of Continuous EEG Monitoring in Neonates: Report of the American Clinical Neurophysiology Society Critical Care Monitoring Committee,” *J. Clin. Neurophysiol.*, vol. 30, no. 2, p. 161, Apr. 2013, doi: 10.1097/WNP.0b013e3182872b24.

[16] “eCFR :: 21 CFR 882.5802 -- Transcranial magnetic stimulation system for neurological and psychiatric disorders and conditions.” Accessed: Sept. 17, 2025. [Online]. Available: https://www.ecfr.gov/current/title-21/chapter-I/subchapter-H/part-882/subpart-F/section-882.5802

[17] *Standard Test Method for Measurement of Radio Frequency Induced Heating On or Near Passive Implants During Magnetic Resonance Imaging*, F2182-19e2.

[18] D. Xie, J. Bian, C. Ni, P. Zhao, Z. Pu, and J. Yue, “Tuning Room-Temperature Injectability of Gelatin-Based Hydrogels via Introduction of Competitive Hydrogen Bonds,” *ACS Macro Lett.*, vol. 14, no. 3, pp. 313–319, Mar. 2025, doi: 10.1021/acsmacrolett.5c00018.

[19] F. Mushtaq *et al.*, “Preparation, properties, and applications of gelatin-based hydrogels (GHs) in the environmental, technological, and biomedical sectors,” *Int. J. Biol. Macromol.*, vol. 218, pp. 601–633, Oct. 2022, doi: 10.1016/j.ijbiomac.2022.07.168.

[20] S. P. Pandey, T. Shukla, V. K. Dhote, D. K. Mishra, R. Maheshwari, and R. K. Tekade, “Chapter 4 - Use of Polymers in Controlled Release of Active Agents,” in *Basic Fundamentals of Drug Delivery*, R. K. Tekade, Ed., in Advances in Pharmaceutical Product Development and Research. , Academic Press, 2019, pp. 113–172. doi: 10.1016/B978-0-12-817909-3.00004-2.

[21] B. Ayyakkalai, J. Nath, H. G. Rao, V. Venkata, S. S. Nori, and S. Suryanarayan, “Chapter 17 - Seaweed derived sustainable packaging,” in *Applications of Seaweeds in Food and Nutrition*, D. I. Hefft and C. O. Adetunji, Eds., Elsevier, 2024, pp. 263–287. doi: 10.1016/B978-0-323-91803-9.00006-8.

[22] F. Jiang *et al.*, “Extraction, Modification and Biomedical Application of Agarose Hydrogels: A Review,” *Mar. Drugs*, vol. 21, no. 5, p. 299, May 2023, doi: 10.3390/md21050299.

[23] “3D Printer Dimensions,” Google Docs. Accessed: Sept. 25, 2025. [Online]. Available: https://docs.google.com/spreadsheets/d/125EWYr0aojDuu0BGfzzt-YhfGJA1wojkzE-Vt00tw_M/edit?gid=0&usp=embed_facebook

[24] M. Nofar, D. Sacligil, P. J. Carreau, M. R. Kamal, and M.-C. Heuzey, “Poly (lactic acid) blends: Processing, properties and applications,” *Int. J. Biol. Macromol.*, vol. 125, pp. 307–360, Mar. 2019, doi: 10.1016/j.ijbiomac.2018.12.002.

[25] “Polylactic Acid (PLA, Polylactide) :: MakeItFrom.com.” Accessed: Oct. 13, 2025. [Online]. Available: https://www.makeitfrom.com/material-properties/Polylactic-Acid-PLA-Polylactide

[26] "Polymethyl Methacrylate - an overview | ScienceDirect Topics." Accessed: Oct. 13, 2025. [Online]. Available: https://www-sciencedirect-com.ezproxy.library.wisc.edu/topics/chemical-engineering/polymethyl-methacrylate
[27] "BioMed Clear Resin," Formlabs. Accessed: Sept. 25, 2025. [Online]. Available: https://formlabs.com/store/materials/biomed-clear-resin/
[28] "Clear Resin," Formlabs. Accessed: Dec. 12, 2025. [Online]. Available: https://formlabs.com/store/materials/clear-resin/
[29] A. Antoniou, N. Evripidou, L. Georgiou, A. Chrysanthou, C. Ioannides, and C. Damianou, "Tumor phantom model for MRI-guided focused ultrasound ablation studies," *Med. Phys.*, vol. 50, no. 10, pp. 5956–5968, Oct. 2023, doi: 10.1002/mp.16480.
[30] X. Xie, D. Li, T.-H. Tsai, J. Liu, P. V. Braun, and D. G. Cahill, "Thermal Conductivity, Heat Capacity, and Elastic Constants of Water-Soluble Polymers and Polymer Blends," *Macromolecules*, vol. 49, no. 3, pp. 972–978, Feb. 2016, doi: 10.1021/acs.macromol.5b02477.
[31] T. Sakiyama, S. Han, A. Torii, O. Miyawaki, and T. Yano, "Intrinsic Thermal Conductivity of Gelatin Estimated Independently of Heat Conduction Models".
[32] E. Myers, M. Piazza, M. Owkes, and R. K. June, "Heat conduction simulation of chondrocyte-embedded agarose gels suggests negligible impact of viscoelastic dissipation on temperature change," *J. Biomech.*, vol. 176, p. 112307, Nov. 2024, doi: 10.1016/j.jbiomech.2024.112307.
[33] A. Sun *et al.*, "Current research progress of photopolymerized hydrogels in tissue engineering," *Chin. Chem. Lett.*, vol. 32, no. 7, pp. 2117–2126, July 2021, doi: 10.1016/j.cclet.2021.01.048.
[34] G. Satchanska, S. Davidova, and P. D. Petrov, "Natural and Synthetic Polymers for Biomedical and Environmental Applications," *Polymers*, vol. 16, no. 8, p. 1159, Apr. 2024, doi: 10.3390/polym16081159.
[35] S. Sharifi *et al.*, "Tuning gelatin-based hydrogel towards bioadhesive ocular tissue engineering applications," *Bioact. Mater.*, vol. 6, no. 11, pp. 3947–3961, Nov. 2021, doi: 10.1016/j.bioactmat.2021.03.042.
[36] "Agar Agar Powder," TM Media. Accessed: Sept. 25, 2025. [Online]. Available: https://www.tmmedia.in/wp-content/uploads/MSDS/MSDS-1201.pdf
[37] M. Earle, G. D. Portu, and E. DeVos, "Agar ultrasound phantoms for low-cost training without refrigeration.," *Afr. J. Emerg. Med. Rev. Afr. Med. Urgence*, vol. 6, no. 1, pp. 18–23, Mar. 2016, doi: 10.1016/j.afjem.2015.09.003.
[38] M.-E. Karga, M.-E. Kargaki, H. Iatrou, and C. Tsitsilianis, "pH-Responsive, Thermo-Resistant Poly(Acrylic Acid)-g-Poly(boc-L-Lysine) Hydrogel with Shear-Induced Injectability.," *Gels Basel Switz.*, vol. 8, no. 12, Dec. 2022, doi: 10.3390/gels8120817.
[39] "Safety Data Sheet (SDS): Poly(acrylic acid)," Chemos. Accessed: Sept. 25, 2025. [Online]. Available: https://www.chemos.de/import/data/msds/GB_en/9003-01-4-A0069730-GB-en.pdf
[40] Z. Zhang, X. Wang, Y. Wang, and J. Hao, "Rapid-Forming and Self-Healing Agarose-Based Hydrogels for Tissue Adhesives and Potential Wound Dressings,"

Biomacromolecules, vol. 19, no. 3, pp. 980–988, Mar. 2018, doi: 10.1021/acs.biomac.7b01764.

[41] "Safety Data Sheet: Agarose Powder," Fisher Scientific. Accessed: Sept. 25, 2025. [Online]. Available: https://www.fishersci.com/content/dam/fishersci/en_US/documents/programs/education/regulatory-documents/sds/chemicals/chemicals-a/S25128.pdf

[42] "Safety Data Sheet (SDS)," ATP Type. Accessed: Sept. 25, 2025. [Online]. Available: https://atpgroup.com/wp-content/uploads/2018/06/Gelatin-Rousselot-SDS.pdf

[43] A. I. Farrer *et al.*, "Characterization and evaluation of tissue-mimicking gelatin phantoms for use with MRgFUS," *J. Ther. Ultrasound*, vol. 3, no. 1, p. 9, June 2015, doi: 10.1186/s40349-015-0030-y.

[44] S. Mad-Ali, S. Benjakul, T. Prodpran, and S. Maqsood, "Characteristics and gelling properties of gelatin from goat skin as affected by drying methods.," *J. Food Sci. Technol.*, vol. 54, no. 6, pp. 1646–1654, May 2017, doi: 10.1007/s13197-017-2597-5.

[45] L. Lépine and R. Gilbert, "Thermal degradation of polyacrylic acid in dilute aqueous solution," *Polym. Degrad. Stab.*, vol. 75, no. 2, pp. 337–345, Jan. 2002, doi: 10.1016/S0141-3910(01)00236-1.

[46] Q.-Q. Ouyang *et al.*, "Thermal degradation of agar: Mechanism and toxicity of products," *Food Chem.*, vol. 264, pp. 277–283, Oct. 2018, doi: 10.1016/j.foodchem.2018.04.098.

[47] L.-M. Zhang, C.-X. Wu, J.-Y. Huang, X.-H. Peng, P. Chen, and S.-Q. Tang, "Synthesis and characterization of a degradable composite agarose/HA hydrogel," *Carbohydr. Polym.*, vol. 88, no. 4, pp. 1445–1452, May 2012, doi: 10.1016/j.carbpol.2012.02.050.

[48] "Great Value Unflavored Gelatin Mix, 0.25 oz, 32 Count Pouches," Walmart.com. Accessed: Oct. 13, 2025. [Online]. Available: https://www.walmart.com/ip/Great-Value-Unflavored-Gelatin-Mix-0-25-oz-32-Count-Pouches/531996398

[49] "Agar powder 500 g | Buy Online | Thermo Scientific Chemicals | thermofisher.com." Accessed: Oct. 12, 2025. [Online]. Available: https://www.thermofisher.com/order/catalog/product/A10752.36

[50] "Agarose, Electrophoresis Grade 250 g | Buy Online | Thermo Scientific Chemicals | thermofisher.com." Accessed: Oct. 13, 2025. [Online]. Available: https://www.thermofisher.com/order/catalog/product/J66501.30

[51] "Poly(acrylic acid) average Mv 3,000,000, powder 9003-01-4." Accessed: Oct. 13, 2025. [Online]. Available: https://www.sigmaaldrich.com/US/en/product/aldrich/306223?srsltid=AfmBOoohEpWt90QcbNACXGLO5NifU4DvKziUsvjTPQ9TChj-B5czavXL

[52] "Ultimate Guide to PMMA/Acrylic Filament 3D Printing - 3DSourced." Accessed: Oct. 13, 2025. [Online]. Available: https://www.3dsourced.com/rigid-ink/pmma-filament-acrylic/

[53] "Dielectric Properties » IT'IS Foundation." Accessed: Oct. 13, 2025. [Online]. Available: https://itis.swiss/virtual-population/tissue-properties/database/dielectric-properties/

[54] “Polymethyl Methacrylate (PMMA) - Properties.” Accessed: Oct. 13, 2025. [Online]. Available: https://matmake.com/materials-data/polymethyl-methacrylate-properties.html
[55] “(PDF) Analysis of FDM and DLP 3D-Printing Technologies to Prototype Electromagnetic Devices for RFID Applications,” *ResearchGate*, Apr. 2025, doi: 10.3390/s21030897.
[56] L. Falland-Cheung, J. N. Waddell, K. Chun Li, D. Tong, and P. Brunton, “Investigation of the elastic modulus, tensile and flexural strength of five skull simulant materials for impact testing of a forensic skin/skull/brain model,” *J. Mech. Behav. Biomed. Mater.*, vol. 68, pp. 303–307, Apr. 2017, doi: 10.1016/j.jmbbm.2017.02.023.
[57] “3D Printers,” Grainger Engineering Design Innovation Lab. Accessed: Sept. 25, 2025. [Online]. Available: https://making.engr.wisc.edu/equipment/3d-printers/
[58] “Additive Manufacturing | 3D Printing Services,” Rapid Prototyping & Low Volume Production. Accessed: Sept. 25, 2025. [Online]. Available: https://www.3erp.com/services/3d-printing/
[59] “Amazon.com: MSNJ PMMA Filament 1.75mm,PMMA 3D Printer Filament,Dimensional Accuracy +/-0.03 mm,1KG(2.2lb)Spool,Transparent : Industrial & Scientific.” Accessed: Sept. 25, 2025. [Online]. Available: https://www.amazon.com/Filament-Printer-Dimensional-Accuracy-Transparent/dp/B08Y5LKNLB
[60] W. Hou *et al.*, “Design of injectable agar/NaCl/polyacrylamide ionic hydrogels for high performance strain sensors,” *Carbohydr. Polym.*, vol. 211, pp. 322–328, May 2019, doi: 10.1016/j.carbpol.2019.01.094.
[61] “Gelatin powder, 300g Bloom, Type A, BioReagent, for electrophoresis, cell culture mammalian 9000-70-8.” Accessed: Dec. 10, 2025. [Online]. Available: https://www.sigmaaldrich.com/US/en/product/sigma/g1890
[62] X. Yan *et al.*, “High strength and self-healable gelatin/polyacrylamide double network hydrogels,” *J. Mater. Chem. B*, vol. 5, no. 37, pp. 7683–7691, Sept. 2017, doi: 10.1039/C7TB01780D.
[63] N. Russ, B. I. Zielbauer, K. Koynov, and T. A. Vilgis, “Influence of Nongelling Hydrocolloids on the Gelation of Agarose,” *Biomacromolecules*, vol. 14, no. 11, pp. 4116–4124, Nov. 2013, doi: 10.1021/bm4012776.
[64] “What is SLA printing? The original resin 3D print method,” Protolabs Network. Accessed: Oct. 12, 2025. [Online]. Available: https://www.hubs.com/knowledge-base/what-is-sla-3d-printing/
[65] A. Amirabdollahian and M. Moeini, “An In Situ-Gelling Conductive Hydrogel for Potential Use in Neural Tissue Engineering,” *Tissue Eng. Part A*, vol. 30, no. 23–24, pp. 726–739, 2024, doi: 10.1089/ten.tea.2023.0359.
[66] J. Yang, H. C. Cramer, E. C. Bremer, S. Buyukozturk, Y. Yin, and C. Franck, “Mechanical characterization of agarose hydrogels and their inherent dynamic instabilities at ballistic to ultra-high strain-rates via inertial microcavitation,” *Extreme Mech. Lett.*, vol. 51, p. 101572, Feb. 2022, doi: https://doi.org/10.1016/j.eml.2021.101572.

A. Product Design Specifications (PDS)

Function

Intracranial electroencephalography (iEEG) is routinely used in surgical planning for individuals with uncontrolled seizures, such as those with epilepsy. Utilizing electrode systems either connected across the surface of or implanted into the brain, this method provides high spatiotemporal resolution [1]. Transcranial magnetic stimulation (TMS) assesses brain circuit excitability through electromagnetic induction, inducing currents to produce action potentials and painlessly activate brain networks [2]. While this neuromodulation technique may provide complementary information for mapping out critical brain regions that should be avoided during surgery, there are several safety concerns around the use of TMS in patients with iEEG: that of secondary electrical currents, heating of the implanted electrodes, and electrode array displacement, all of which would have severe consequences for the affected individuals [1]. Additionally, the impact of these techniques has not been previously studied on children with epilepsy, but instead on adult patients; dissimilar physiology and comparative higher resting motor thresholds might require higher levels of stimulation, both of which indicate the need for adjusted treatment [3]. The goal of this project, therefore, is to develop a pediatric brain phantom model that can be used to simulate the main effects of TMS on iEEG electrodes: currents, temperatures, and changes in position.

Client requirements

1. The phantom should represent the physiology of the pediatric brain in terms of overall matter volume, approximately 1300 mm^3, and circumference of the surrounding skull, between 50 to 54 cm [4], [5].
2. The material should have efficient conductivity to allow for proper current testing; to represent brain tissue conductivity, this value should lie between 0.2 and 0.5 S/m [6].
3. The device must be able to withstand a minimum of 50 magnetic pulses, as is common in TMS sessions for human participants [1].
4. The phantom must not physically interfere with TMS coil application to allow for adequate testing. To allow for optimal orientation, the TMS operator should be able to hold the coil within 5.5 ± 1.6 mm of the scalp [7].
5. The budget must not exceed $500.

Design requirements

1. Physical and Operational Characteristics

a. Performance requirements

i. The phantom must withstand magnetic pulses up to a frequency of 0.5 Hz, as performed in a previous TMS study on patients with implanted electrodes [1].

ii. To reflect the higher motor threshold present in a pediatric nervous system, as the corticospinal tract continues to develop, the phantom should tolerate pulses up to 2T in magnitude [8], [9].

iii. Similar physiological properties to the young child brain are ideal, including an overall brain matter volume between 50 and 100 mm^3 and appropriate conductivity levels in the range of 0.2 to 0.5 S/m [4], [5].

iv. The shape and structure of the model must be maintained despite implantation of electrode arrays – up to 90 mm [1].

v. The construction of the phantom and any necessary container must allow for measurements of displacement, temperature change, and induced current; as such, the device should be accessible from several points, such as from each of the embedded electrodes.

b. Accuracy and Reliability

i. After treatment with TMS, the implanted electrodes should experience <1°C of heating [10].

ii. The iEEG electrodes should experience displacement of less than 20 mm, as some deformations of the brain can naturally occur [11]. Ideally, there will be no significant displacement.

iii. Charge density must be less than 30 $\mu C/cm^2$ when TMS is being administered at full power [1].

c. Life in Service

i. The phantom will be used to ensure the safety of TMS being used with iEEG technology.

ii. The phantom must be constructed from material that will not degrade over the entire testing period, such as a 3D printed acrylic polymer. The client will define the length of time in vitro testing with the phantom will occur.

iii. Each round of TMS testing will last approximately 350 seconds [12].

d. Shelf Life

i. The shelf life necessary for this phantom will extend for the duration of client testing. After in vitro testing is complete, the client will begin clinical trials with pediatric patients.

ii. To ensure minimal material degradation, the phantom will be stored at room temperature and humidity, 22-24 °C and 40-60%, respectively [13].

iii. Depth electrodes will be used. They will not be permanently implanted but should be used within approximately 3 years [14].

e. Operating Environment

i. The phantom will be used in conjunction with TMS and iEEG technology. Materials must be compatible with this technology.
ii. The phantom will be used in a sterile environment and handled by neurosurgeons during testing.
iii. The phantom will be used at average room temperature, 22-24 ℃, and humidity, 40-60% [13].

f. Ergonomics

i. Neurosurgeons handling the phantom must be able to safely use and replace components of the phantom, such as the gel and electrodes, between testing.
ii. The phantom will be placed on a table for the duration of testing, approximately 1 meter (m) off the ground.

g. Size

i. The phantom should mimic the size of an average pediatric brain and skull.
ii. The approximate volume of the phantom will be 50-100 mm^3 [4].
iii. The approximate circumference of the skull of the phantom will be 50-54 cm [5].

h. Weight

i. The phantom will ideally be less than 2 kg to ensure the phantom is easy to transport and lift without causing strain to the user.

i. Materials

i. The base of the phantom will be constructed from a 3D printed acrylic polymer. Acrylic based filament or resin for 3D printing has good optical clarity for viewing access into the phantom and good durability. 3D printed polymethyl methacrylate (PMMA) parts showed minimal degradation over 5 years [15].
ii. 6-12 contact EEG electrodes will be embedded in silicone for precise positioning of the implanted electrodes [1]. Depth arrays (platinum macro contacts) are implanted while grid arrays (platinum-iridium) are placed on the cortical surface [12].
iii. A hydrogel will be used to approximate brain tissue. Similar phantoms have used a polyacrylic acid saline gel [1], agar, gelatin, or agarose. The addition of NaCl is necessary to achieve physiologically accurate electrical conductivity [16].
iv. Fiberoptic fluorescent temperature sensors can be connected perpendicular to the electrodes to measure changes in temperature [12].
v. Ferromagnetic materials will be avoided so as to not interfere with the TMS induced magnetic field [17].

j. Aesthetics, Appearance, and Finish

i. The base of the phantom should be 3D printed from a clear filament/resin so that the implanted electrodes and internal components can be easily viewed.

ii. A replaceable hydrogel brain mimics the texture and conductive properties of the brain. However, a gel with greater optical clarity is desired for positioning and viewing the electrodes.
iii. A gel-based phantom housed in a rectangular box is better for calibration testing and can be used to evaluate temperature changes and basic electromagnetic effects of TMS [18].
iv. A skull-based phantom would provide greater anatomical accuracy and more complex geometry is important to evaluate TMS induced fields more realistically [19]. Therefore a combination approach will be taken, where a simpler gel-box phantom will be created for initial testing, before moving onto a more complex skull-based phantom.

2. Production Characteristics

a. Quantity

i. The client desires one gel based phantom housed in a 3D printed rectangular box to first be created for preliminary testing before progressing to a skull-based phantom for improved accuracy.

b. Target Product Cost

i. The total production cost must not exceed the budget of $500.

3. Miscellaneous

a. Standards and Specifications

i. MTR Standards 2.4 and 3.3 require pediatric patients with implanted electrodes to have an inter-electrode impedance of up 10 kOhms maximum, and that electroencephelograms be run with a reduced sensitivity of 7 microvolts (uV), respectively [20].
ii. CFR Standard 882.5802 defines the use of TMS coils for treatment of neurological and psychiatric disorders as Class II medical devices with specific controls. Therefore, the testing procedure defined must consider magnetic pulse output, magnetic and electrical field, built in device safety features, and patient exposure to sound during device use [21].
iii. The testing of the phantom must follow ASTM standard F2182, which details a test procedure for measuring temperature change due to induced current during magnetic resonance applied to implanted devices [22].

b. Customer

i. The customers for this project are pediatric patients with intracranial implanted electrodes who will need to undergo neurosurgery.

c. Patient-related concerns

i. Patient-related concerns during simultaneous iEEG and TMS include heating of electrodes, induced electrical current, and displacement of electrodes. This phantom will investigate the likelihood and severity of each of these concerns on a pediatric patient.

d. Competition

i. A similar phantom used to test the safety of combined iEEG and TMS was recently made at the University of Iowa [1]. This phantom used a polyacrylic acid (PAA) gel base with a polymethyl methacrylate (PMMA) wall, representing the brain and skull tissue, respectively. This phantom was successfully used to verify safety of concurrent iEEG and TMS use in adult patients undergoing treatment for neuropsychiatric disorders. While this phantom addresses many of the current project's concerns, it fails to account for more stringent safety standards and physiological differences required when considering pediatric patients.

PDS References

[1] J. B. Wang *et al.*, "Effects of transcranial magnetic stimulation on the human brain recorded with intracranial electrocorticography," *Mol. Psychiatry*, vol. 29, no. 5, pp. 1228–1240, May 2024, doi: 10.1038/s41380-024-02405-y.

[2] J.-P. Lefaucheur, "Chapter 37 - Transcranial magnetic stimulation," in *Handbook of Clinical Neurology*, vol. 160, K. H. Levin and P. Chauvel, Eds., in Clinical Neurophysiology: Basis and Technical Aspects, vol. 160. , Elsevier, 2019, pp. 559–580. doi: 10.1016/B978-0-444-64032-1.00037-0.

[3] E. N. Sutter, C. P. Casey, and B. T. Gillick, "Single-pulse transcranial magnetic stimulation for assessment of motor development in infants with early brain injury," *Expert Rev. Med. Devices*, vol. 21, no. 3, pp. 179–186, Mar. 2024, doi: 10.1080/17434440.2023.2299310.

[4] R. a. I. Bethlehem *et al.*, "Brain charts for the human lifespan," *Nature*, vol. 604, no. 7906, pp. 525–533, Apr. 2022, doi: 10.1038/s41586-022-04554-y.

[5] "Head circumference for age." Accessed: Sept. 13, 2025. [Online]. Available: https://www.who.int/tools/child-growth-standards/standards/head-circumference-for-age

[6] G. Halnes, T. V. Ness, S. Næss, E. Hagen, K. H. Pettersen, and G. T. Einevoll, *Electric Brain Signals: Foundations and Applications of Biophysical Modeling*, 1st ed. Cambridge University Press, 2024. doi: 10.1017/9781009039826.

[7] J. Gomez-Tames, A. Hamasaka, I. Laakso, A. Hirata, and Y. Ugawa, "Atlas of optimal coil orientation and position for TMS: A computational study," *Brain Stimulat.*, vol. 11, no. 4, pp. 839–848, July 2018, doi: 10.1016/j.brs.2018.04.011.

[8] M. Q. Hameed *et al.*, “Transcranial Magnetic and Direct Current Stimulation in Children,” *Curr. Neurol. Neurosci. Rep.*, vol. 17, no. 2, p. 11, Feb. 2017, doi: 10.1007/s11910-017-0719-0.

[9] “TMS (Transcranial Magnetic Stimulation): What It Is,” Cleveland Clinic. Accessed: Sept. 14, 2025. [Online]. Available: https://my.clevelandclinic.org/health/treatments/17827-transcranial-magnetic-stimulation-tms

[10] Y. Fujita *et al.*, “Evaluating the Safety of Simultaneous Intracranial Electroencephalography and Functional Magnetic Resonance Imaging Acquisition Using a 3 Tesla Magnetic Resonance Imaging Scanner,” *Front. Neurosci.*, vol. Volume 16, June 2022, doi: 10.3389/fnins.2022.921922.

[11] A. O. Blenkmann *et al.*, “Anatomical registration of intracranial electrodes. Robust model-based localization and deformable smooth brain-shift compensation methods.,” May 11, 2023, *United States*. doi: 10.1101/2023.05.08.539503.

[12] J. B. Wang *et al.*, “Supplementary information to ‘Effects of transcranial magnetic stimulation on the human brain recorded with intracranial electrocorticography.’” 2024. [Online]. Available: https://static-content.springer.com/esm/art%3A10.1038%2Fs41380-024-02405-y/MediaObjects/41380_2024_2405_MOESM1_ESM.pdf

[13] “Humidity for Hospital and Healthcare Facilities.” Accessed: Sept. 14, 2025. [Online]. Available: https://www.neptronic.com/humidifiers/pdf/flyers/Flyer_Humidity%20for%20Hospitals%20&%20Healthcare_EN_20220527.pdf

[14] “DEN-12SAF: EEG Needles, 12mm x 29 gauge, 48",” Electrode Store. Accessed: Sept. 17, 2025. [Online]. Available: https://electrodestore.com/products/den-12-needles?variant=18289707155518&country=US&currency=USD&utm_medium=product_sync&utm_source=google&utm_content=sag_organic&utm_campaign=sag_organic&srsltid=AfmBOoojIjxe9i01ONswFljvcAeHpmp2qTiUnwBij6mg3NrGei-Y5iDcwEA

[15] J. C. Raffaini *et al.*, “Effect of artificial aging on mechanical and physical properties of CAD-CAM PMMA resins for occlusal splints,” *J. Adv. Prosthodont.*, vol. 15, no. 5, pp. 227–237, Oct. 2023, doi: 10.4047/jap.2023.15.5.227.

[16] M. A. Kandadai, J. L. Raymond, and G. J. Shaw, “Comparison of electrical conductivities of various brain phantom gels: Developing a ‘Brain Gel Model,’” *Mater. Sci. Eng. C Mater. Biol. Appl.*, vol. 32, no. 8, pp. 2664–2667, Dec. 2012, doi: 10.1016/j.msec.2012.07.024.

[17] S. Rossi *et al.*, “Safety and recommendations for TMS use in healthy subjects and patient populations, with updates on training, ethical and regulatory issues: Expert Guidelines,” *Clin. Neurophysiol. Off. J. Int. Fed. Clin. Neurophysiol.*, vol. 132, no. 1, pp. 269–306, Jan. 2021, doi: 10.1016/j.clinph.2020.10.003.

[18] A. Antoniou *et al.*, “MR relaxation times of agar-based tissue-mimicking phantoms,” *J. Appl. Clin. Med. Phys.*, vol. 23, no. 5, p. e13533, 2022, doi: 10.1002/acm2.13533.

[19] H. Magsood and R. L. Hadimani, “Development of anatomically accurate brain phantom for experimental validation of stimulation strengths during TMS,” *Mater. Sci. Eng. C*, vol. 120, p. 111705, Jan. 2021, doi: 10.1016/j.msec.2020.111705.

[20] T. N. Tsuchida *et al.*, “American Clinical Neurophysiology Society Standardized EEG Terminology and Categorization for the Description of Continuous EEG Monitoring in Neonates: Report of the American Clinical Neurophysiology Society Critical Care Monitoring Committee,” *J. Clin. Neurophysiol.*, vol. 30, no. 2, p. 161, Apr. 2013, doi: 10.1097/WNP.0b013e3182872b24.

[21] “eCFR :: 21 CFR 882.5802 -- Transcranial magnetic stimulation system for neurological and psychiatric disorders and conditions.” Accessed: Sept. 17, 2025. [Online]. Available: https://www.ecfr.gov/current/title-21/chapter-I/subchapter-H/part-882/subpart-F/section-882.5802

[22] *Standard Test Method for Measurement of Radio Frequency Induced Heating On or Near Passive Implants During Magnetic Resonance Imaging*, F2182-19e2.

B. Processing CT Scans in 3D Slicer

1. Open 3D Slicer → Load DICOM file.
2. Go to “Segment Editor”.
3. Add a new segment → choose “Threshold”.
4. Use slider to find bone thresholds (~150-3000 HU) and apply.
5. Preview model and refine using tools like:
    a. Smoothing.
    b. Islands → Keep largest.
    c. Scissors/Paint for manual cleanup.
6. When satisfied: Segmentations → Export to 3D Model.
    a. STL for direct 3D printing.
    b. STL or OBJ for conversion to CAD software such as SolidWorks.
    c. NRRD if uploading to any place that patient data needs to be anonymized.

C. Processing STL Files into Workable CAD Files

File processing from STL to CAD:

1. Obtain STL file or process DICOM file into STL (see procedure for doing this in 3D Slicer).
2. Import STL file into Fusion360.
3. Manually remove any artifacts from scan (this can also be done in 3D slicer before exporting as an STL file).
4. Use repair mesh → close holes, wrap, and stitch and remove.
5. Compress model to smaller ratio to avoid crashing with larger file.
6. Generally, want less than 50k triangles. The smaller the number the better, but with more compression detail is lost.
7. Convert mesh to solid body (prismatic).
8. Export as STEP file.
    a. Or to stay in Fusion360 to edit the CAD model stop here!
9. Import STEP file into SolidWorks
    a. This step can take around 30 minutes to import, especially if the file has a lot of triangles
    b. Use internal repair tools to fill any remaining gaps.
10. Save as a SLDPRT (part) file.

To edit the CAD file:

1. Create a sketch on the surface.
    a. May be necessary to create a plane along the surface by creating individual points and anchoring them to the surface
    b. SolidWorks is nice because it allows for the creation of 3D sketches, one reason to use it over Fusion360.
2. Extruded cut from sketch to create top half of the skull.
3. Save a separate copy of the same file.
4. Reverse the extruded cut to leave the bottom half of the skull.
5. Additional extruded cuts to remove any undesirable components.
6. Save both files and export them as STL or STEP file for 3D printing.

D. Hydrogel Fabrication Process

Gelatin Hydrogel

Materials:

- Type I gelatin powder (MilliPore Sigma)
- NaCl powder (Fisher Scientific)
- MilliQ deionized water

Methods:

1. Make a 0.17% saline solution by adding NaCl powder to deionized water at 60 ℃, 300 RPM until completely dissolved.
2. Add appropriate amount of gelatin powder to reach a 6% solution and continue to dissolve on a hot plate set to 60 ℃, until the mixture is transparent. This should take about 30 minutes.
3. Once dissolved, pour gelatin mixture into clean molds and cool in 4 ℃ fridge until set.

Agar Hydrogel

Materials:

- Agar powder (Thermo Scientific)
- NaCl powder (Fisher Scientific)
- MilliQ deionized water

Methods:

1. Make a 0.17% saline solution by adding NaCl powder to deionized water at 60 ℃, 300 RPM until completely dissolved.
2. Add appropriate amount of agar powder to reach 1.2% solution and continue to dissolve on a hot plate at 80 ℃ until completely dissolved. This should take about 20 minutes.
3. Once dissolved, pour agar mixture into clean molds and set at room temperature overnight.

E. Shrink-Swell Testing Protocol

Materials:

- Prepared hydrogel of varying concentrations
    - DI water
    - Hydrogel powder
    - NaCl powder
- Cylindrical cutting tool
- 100% EtOH
- Timer
- Weigh boats
- 50 mL beakers
- Analytical scale

Methods:

1. Label 50 mL beakers, at least 3 for each hydrogel concentration group
2. Place 10 mL 100% EtOH in each beaker
3. Cut uniform discs for each hydrogel sample that will fit into the labeled beakers
4. Record initial weights for each sample
5. Place each sample into its own beaker and begin a stopwatch
6. Record mass measurements every 20 minutes until 60 minutes have passed
7. Record final mass at 60 minutes
8. Replace EtOH with DI water in each beaker
9. After approximately 1 day has passed, record final swelled mass of the hydrogel

F. MATLAB for Shrink-Swell Statistics

```
%% BME 400 Shrink Swell Stats
data = readtable("Agar_ShrinkSwell_Stats.csv");

%final vs initial values across concentrations(0 min vs 60 min)
initial_0_5 = [data{1, "x0_5_n1"} data{1, "x0_5_n2"} data{1, "x0_5_n3"}];
initial_1 = [data{1, "x1_0_n1"} data{1, "x1_0_n2"} data{1, "x1_0_n3"}];
initial_1_5 = [data{1, "x1_5_n1"} data{1, "x1_5_n2"} data{1, "x1_5_n3"}];

final_0_5 = [data{4, "x0_5_n1"} data{4, "x0_5_n2"} data{4, "x0_5_n3"}];
final_1 = [data{4, "x1_0_n1"} data{4, "x1_0_n2"} data{4, "x1_0_n3"}];
final_1_5 = [data{4, "x1_5_n1"} data{4, "x1_5_n2"} data{4, "x1_5_n3"}];

all_initial = [initial_0_5; initial_1; initial_1_5];
all_final = [final_0_5; final_1; final_1_5];

pct_change1 = (all_final - all_initial) ./ all_initial * 100;
test1 = pct_change1(:);
group = ["0.5%";"1.0%";"1.5%";"0.5%";"1.0%";"1.5%";"1.0%";"1.0%";"1.5%"];
p1 = anova1(test1, group);
%p = 0.4176, not significant at all

%significance initial mass vs rehydrated comparing concentrations
reswell_0_5 = [data{5, "x0_5_n1"} data{5, "x0_5_n2"} data{5, "x0_5_n3"}];
reswell_1 = [data{5, "x1_0_n1"} data{5, "x1_0_n2"} data{5, "x1_0_n3"}];
reswell_1_5 = [data{5, "x1_5_n1"} data{5, "x1_5_n2"} data{5, "x1_5_n3"}];

all_reswell = [reswell_0_5; reswell_1; reswell_1_5];

pct_change2 = (all_reswell - all_initial) ./ all_initial * 100;
test2 = pct_change2(:);
p2 = anova1(test2,group);
%p = 0.0828, not significant but closer than the other

%% Paired T-Tests 0 vs 60 Minutes of Agar Shrink-swell
% load data
table = (AgarShrinkSwellTestingS4);
data = table2array(table);

% define variables for time 0 and time 60 minutes for each condition
t0_5 = data(2, 2:4);
t60_5= data(5, 2:4);

t0_1 = data(2, 5:7);
t60_1= data(5, 5:7);

t0_15 = data(2, 8:10);
t60_15= data(5, 8:10);
```

```
% run a paired t test on the overall data sets
[h5, p5] = ttest(t0_5, t60_5)
% h=0, p=0.0798

[h1, p1] = ttest(t0_1, t60_1)
% h=1, p=0.0053

[h15, p15] = ttest(t0_15, t60_15)
%h=1, p=0.0110
```

G. Arduino IDE Code for Temperature Measurements

```
int sensorPin = A0;    // select the input pin
int sensorValue = 0;  // variable to store value coming the sensor
float tempSum = 0.0;
int count = 0;

void setup() {
  Serial.begin(9600);
}
void loop() {
  // read the value from the sensor:
  sensorValue = analogRead(sensorPin);
  float voltage = (sensorValue * 0.0049);
  float temp = (voltage + 0.267) / 0.0143;

  count++;
  tempSum = tempSum + temp;
  float temp_ave;
  if (count == 100) {
    temp_ave = (tempSum/100);
    Serial.println(temp_ave);
    tempSum = 0;
    count = 0;
  }
  delay(10);
}
```

H. MATLAB Script for Calculating Thermal Conductivity and Statistics

```
%% BME400 Thermal Conductivity Stats
table = readtable("ThermalConductivityTemperatureTestingDataS2");
data = table2array(table);
m= data(:, 7) ./ 1000;
c= [4;4;4;4;4;4;4;4;4] .*1000;
dTemp = data(:, 8);
dtime = [600;600;600;600;600;600;600;600;600];
x = data(:, 4) ./100;
A = data(:,3) ./ 10^4;
T = 35 - (data(:, 5));
percentgelatin = data(:, 2);

thermal_conductivity = (m.*c.*(dTemp./dtime).*x)./(A.*T);

TC4 = thermal_conductivity(1:3, :);
TC6 =  thermal_conductivity(4:6,:);
TC8 = thermal_conductivity(7:9,:);

all = [TC4; TC6; TC8];
groups = ["4%"; "4%";"4%";"6%";"6%";"6%";"8%";"8%";"8%"];
p = anova1(all,groups);
%p = 0.082, not significantly different across groups

a4 = mean(TC4);
s4 = std(TC4);
m4 = median(TC4);

a6 = mean(TC6);
s6 = std(TC6);
m6 = median(TC6);

a8 = mean(TC8);
s8 = std(TC8);
m8 = median(TC8);

figure(1)
boxplot(thermal_conductivity, percentgelatin, 'Labels', {'4% Gelatin', '6%
Gelatin', '8% Gelatin'})
title("Thermal Conductivities of Various Gelatin Concentrations", "FontSize",
16)
ylabel('Thermal Conductivity (W/m-K)', "FontSize", 16)
```

I. Thermal Conductivity Testing Protocol

Materials:

- Prepared hydrogel of varying concentrations
    - DI water
    - Hydrogel powder
    - NaCl powder
- Scalpel
- Ruler/Calipers
- Large Kimwipe
- Hotplate
- Ring Stand
- K-Type Thermocouple
- LT1025 Cold Junction
- μA741 Operational Amplifier
- Resistors (1 kΩ and 330 kΩ)
- Capacitors (0.1 μF)
- Arduino Uno
- Computer to run Arduino IDE and MATLAB

Methods:

1. Cut prepared hydrogels into rectangular shape and take height, width, and length measurements
2. Turn the hotplate on and set it to 35 ℃
3. Wrap the hydrogel sample in a folded over Kimwipe and secure with tape
4. Mark how far the thermocouple will be inserted and measure the depth
5. Compile and upload Arduino code to begin gathering temperature data
6. Insert the thermocouple into the hydrogel sample and record the initial temperature measurement
7. Place the sample onto the warmed hotplate and begin a stopwatch
8. After 5 minutes have passed, record the temperature
9. Once 10 minutes have passed, record the temperature, and remove the sample from the hotplate
10. Wipe away any residual melted material
11. Repeat steps 3-10 for remaining samples
12. Load gathered data into MATLAB to calculate thermal conductivity for each group

J. Electrical Conductivity Testing Protocol

Materials:

- Keysight E3631A DC power supply
- Two power cables
- Jumper wires
- Alligator clips
- Plastic box container (3 x 3 x 6 cm)
- Drill
- Digital multimeter with two test lead probes
- Fabricated gelatin gels of varying concentrations

Methods:

1. First, make the housing for the gels using the plastic container(s) and a drill. Drill a hole on each end of the length of the container to allow for later jumper wire and multimeter probe insertion.
2. After ensuring that all necessary power supply and measuring components are accessible, fabricate gels of desired concentrations and leave to set overnight at a temperature between 1°C to 4°C.
3. Collect the starting volumetric and mass measurements of gels to be tested.
4. Fit within the housing, ensuring there are no gaps.
5. Before turning on the DC power supply, connect the two power cables – one to the positive power output and one to ground.
6. Connect the cable endpoints to alligator clips, then to two individual jumper wires.
7. Fit the jumper wires into either end of the gel casing, followed by the probes of the digital multimeter.
8. Begin by setting the DC power supply to output 1 V while keeping the current limit to 0. Then, slowly increase the current output to 1 A while monitoring on the digital multimeter.
9. Measure the voltage across the “resistor”, or the gelatin housed within its casing.

K. Shrink-Swell Raw Data

		weight (g)		
Time Point	**n**	**0.50%**	**1.00%**	**1.50%**
initial	1	1.004	1.216	1.192
	2	1.005	1.25	1.17
	3	1.003	1.158	1.07
Addition of 10 mL 200 proof EtOH				
20 min	1	0.9131	0.9087	0.9031
	2	0.8386	0.9341	0.921
	3	0.6335	0.9061	0.9096
40 min	1	0.876	0.8928	0.8742
	2	0.806	0.9262	0.9062
	3	0.592	0.9	0.8688
60 min	1	0.8274	0.8821	0.871
	2	0.7502	0.9261	0.8865
	3	0.5211	0.8959	0.8489
% decrease	1	17.58964143	27.45888158	26.9295302
	2	25.17412935	25.92	24.23076923
	3	48.04586241	22.63385147	20.6635514
Final mass	1	1.1626	1.4952	1.3492
	2	1.0917	1.4675	1.3495
	3	1.1583	1.3926	1.206
% change	1	960817.25%	226238.51%	137657.01%
final vs initial	2	15.80%	22.96%	13.19%
swell	3	8.63%	17.40%	15.34%
	avg	320280.56%	75426.29%	45895.18%
	std	554721.05%	130607.22%	79468.08%

L. Thermal Conductivity Raw Data

Time Point	n	4%	6%	8%
0 sec	1	20.6		20.1
	2	19.6	16.7	20.6
	3	18.67	17.7	21.1
	4	18.7		
	5		19.9	
5 min	1			24.3
	2	20.5	20.5	23.9
	3	24.2	22.5	24.6
	4	23.4		
	5		25.5	
10 min	1			26.1
	2	21.2	22.5	25.6
	3	26	24.8	26.2
	4	25.5		
	5		27.4	
heating plate at 35 deg C				
	sample not used			

Sample ID	Percent Gelatin	Surface Area (cm^2)	X (cm)	Starting temp (C)	Ending temp (C)	Mass (g)	D_temp (C)	Width (cm)	Length (cm)	Height (cm)	Mass(g)
402	4	4.56	1.7	19.6	21.2	10.98	1.6	2.3	3.8	1.2	10.98
403	4	6	0.7	18.67	26	11.51	7.33	2.2	4	1.5	11.51
404	4	6.15	0.5	18.7	25.5	12.39	6.8	2	4.1	1.5	12.39
602	6	2.04	1.3	16.7	22.5	6.81	5.8	2.1	1.7	1.2	6.81
603	6	5.6	2	17.7	24.8	6.4	7.1	2.8	3.5	1.6	6.4
605	6	3.6	0.8	19.9	27.4	6.16	7.5	1.6	2.4	1.5	6.16
801	8	5.1	0.9	20.1	26.1	10.61	6	2	3.4	1.5	10.61
802	8	4.95	1.1	20.6	25.6	10.52	5	2.2	3.3	1.5	10.52
803	8	5.1	0.9	21.1	26.2	8.44	5.1	2	3.4	1.5	8.44

M. BPAG Expense Sheet

Item	Description	Manufac-turer	Mft Pt#	Vendor	Vendor Cat#	Date	#	Cost Each	Total	Link
3D prints										
Formlabs BioMed Clear Sample Swatch	Step wedge with thicknesses of 0.1, 0.2, and 0.3 inches for prelim presentation prop	UW Design and Innovation Lab	N/A	N/A	N/A	10/1	1	$7.14	$7.14	
Rectangular Box Phantom	Box to hold gel for potential displacement testing and poster presentation	UW Design and Innovation Lab	N/A	N/A	N/A	11/21	1	$3.16	$3.16	
Half Scale Skull Phantom	50% scale skull phantom for poster presentation demonstration	UW Design and Innovation	N/A	N/A	N/A	11/24	1	$1.66	$1.66	
Hydrogel Materials										
Agar Powder, 500g	500g of agar powder for initial brain phantom fabrication	Thermo Fisher Scientific	A10752.36	Thermo Fisher Scientific	A10752.36	10/20	1	$128.65	$149.15	https://www.thermofisher.com/order/catalog/product/A10752.36
Gelatin Type A, 100g	100g of Type A gelatin powder from porcine skin for brain phantom fabrication	Millipore Sigma	9000-70-8	Sigma Aldrich	G1890	11/25	1	$53.40	$53.40	https://www.sigmaaldrich.com/US/en/product/sigma/g1890
Food grade gelatin	Food grade gelatin found in teaching lab used for gelatin screening tests	Knox	N/A	BME Teaching Lab	N/A	N/A	1	$0.00	$0.00	
								TOTAL:	**$214.51**	